Peer-reviewed version: *Journal of Scientific and Mathematical Research* **6** (2026) pp. 15-64
jscimath/pubs/J202606-015TM.pdf

Continuous analytical elasticity solutions for arbitrary cross-sections and combined loads

Thad S. Morton

A geometrically exact formulation of three-dimensional elasticity is presented in which coupled translational and rotational deformation is represented within a special Euclidean group SE(3) configuration field defined over the material body. Each material point is represented as an element of SE(3), and the continuum is described by a smooth configuration map whose local strain is obtained via the left-trivialized Maurer–Cartan form. This yields a Lie-algebra-valued strain field capable of describing coupled rotational and translational deformation modes in a unified manner. The configuration is defined by a first-order SE(3) evolution equation whose solution is equivalently represented by a path-ordered exponential of the strain field, providing exact nonlinear reconstruction of the deformed geometry. Constitutive response is formulated directly on the SE(3) strain space using only the material parameters Young's modulus E and shear modulus G. All classical sectional stiffness measures, such as axial stiffness EA, bending stiffness EJ, and torsional stiffness GJ, arise as geometric moment invariants of the cross-section under the SE(3)-induced strain field rather than by being introduced as constitutive inputs. A unified force–moment resultant (wrench) is obtained as the dual of an affine strain measure, providing a direct analytical relation between stress fields without explicit use of moment arms. Classical beam and rod theories, including torsion, bending, axial deformation, and Saint-Venant warping, are recovered as special cases of the general SE(3) formulation. For noncircular cross-sections, warping arises naturally from compatibility conditions expressed in differential form on the SE(3) strain field. The formulation identifies the centroid as the natural reference point for the affine strain measure, eliminating first-moment coupling terms and providing a canonical gauge for the cross-sectional representation.

1. Background

1.1. Elasticity Formulations

Elasticity formulations can be broadly grouped into four distinct approaches. The first, *classical Cauchy elasticity*, describes deformation through displacement gradients, leading to linear theories for small strains (see, e.g., Gere and Timoshenko 1990) and nonlinear finite-deformation models based on tensors such as Green–Lagrange strain. Classical elasticity defines strain first and constructs motion afterwards. Rotation is not treated as an independent geometric variable but is instead uncovered indirectly through the displacement gradient and extracted via antisymmetric or polar components of the deformation tensor. So rotation is not independent; it is derived from spatial gradients of displacement. This is limiting, for example, when a material particle undergoes pure rotation or little or no translation (Bower 2010, Chapter 3). Therefore, it becomes awkward for finite rotations (Antman 2005), rod/shell theories, soft robotics, and independent spin structures (Eringen 1999). Classical beam formulations of elasticity and beam theory rely on small-strain

approximations and linearized rotational kinematics, so while effective for certain problems, they are limited when dealing with bodies undergoing large deformations.

Nomenclature

$\mathbf{a} = \int_0^z \mathbf{\Theta}\boldsymbol{\epsilon}\mathrm{d}s$	translational position of the local frame in field $\mathbf{X}$ [m] (5), (31)
$\beta(z) = \int_0^z \kappa_x(z)\mathrm{d}z$	bending angle [radians] (63), (147)
$\boldsymbol{\epsilon} = \mathbf{\Theta}^{-1}\nabla\mathbf{a}$	translational strain (3×3 matrix) [dimensionless] (22)
$\epsilon_3^{(\mathrm{w})}$	axial displacement due to axial warping during torsion (131)
$\mathbf{G}_x = \begin{bmatrix} 0 & 0 & 0 \\ 0 & 0 & 1 \\ 0 & -1 & 0 \end{bmatrix}$	A basis element of the Lie algebra of rotations (bending about x), also called curvature generator
$\mathbf{G}_z = \begin{bmatrix} 0 & -1 & 0 \\ 1 & 0 & 0 \\ 0 & 0 & 0 \end{bmatrix}$	A basis element of the Lie algebra of rotations (torsion about z), also called curvature generator
$\boldsymbol{\eta}_i = \mathbf{\Gamma}_{,i}\mathbf{R} + \boldsymbol{\epsilon}_{,i}$	constitutive strain, affine strain measure [dimensionless] (36)
$\kappa_B = \partial_z\beta = \partial\beta/\partial z$	curvature due to bending [1/m] (61),
$\kappa_T = \partial_z\phi = \partial\phi/\partial z$	curvature due to torsion (torsional twist density τ) [1/m] (79)
$\mathbf{\Gamma} = \kappa_x\mathbf{G}_x + \kappa_y\mathbf{G}_y + \phi'\mathbf{G}_z$	rotational strain gradient matrix / curvature matrix [1/m] / curvature-twist tensor / matrix representation of the Darboux vector
$\boldsymbol{\kappa} = \begin{bmatrix} \kappa_x \\ \kappa_y \\ \phi' \end{bmatrix} = \mathbf{\Gamma}^\vee$	Darboux vector ("vectorized" curvature matrix) [1/m]
$\mathbf{M}$	moment applied as an external boundary condition [N·m] (53)
$\boldsymbol{\mu}$	moment flux [N/m] (54)
$\mathbf{p} = \mathbf{X}\,\mathbf{r}$	current point obtained from reference point $\mathbf{r}$ by deformation. (4), (148)
$\mathbf{\Pi}$	wrench: moment [N·m] and force [N] (42)
$\phi(z) = \int_0^z \phi'(z)\mathrm{d}z$	torsional rotation angle / orientation [radians]
$\mathbf{\Phi} = \int_0^z \mathbf{\Gamma}(s)\mathrm{d}s$	accumulated curvature matrix / angle matrix [dimensionless]
$\mathbf{\Theta}(z) = e^{\mathbf{\Phi}}$	rotation matrix (operator) [dimensionless] (29)
$\mathbf{r}$	position of a point relative to the coordinate origin [m]
$\mathbf{R}$	position of a point relative to a section centroid [m] (35)
$\boldsymbol{\sigma}$	stress [Pa] (50)
w	strain energy density [Pa] (39)
$\mathbf{X} = \begin{bmatrix} \mathbf{\Theta} & \mathbf{a} \\ 0 & 1 \end{bmatrix}$	configuration of points in a body [m/m m] (3)
$\boldsymbol{\xi} = \begin{bmatrix} \mathbf{\Gamma} & \boldsymbol{\epsilon} \\ 0 & 1 \end{bmatrix}$	exact intrinsic local strain generator [1/m m/m] (20)
$\boldsymbol{\zeta} = (\mathbf{\Theta} - \mathbf{I})\mathbf{r} + \mathbf{a}$	material point displacement [m] (7)
$\mathrm{d}\boldsymbol{\zeta}$	physical strain [m] (149)

A second class of elasticity formulation comprises Cosserat and micropolar continua, where independent rotational degrees of freedom are introduced alongside translations (Cosserat & Cosserat 1909; Eringen 1999). *Cosserat rod theory* (sometimes called Kirchhoff/ Cosserat rod theory) was developed so that large deformations and large rotations can be represented. Strain measures combine displacement gradients with microrotation fields, enabling couple stresses and microstructure-dependent effects (see also Vardoulakis 2019).

A third class, born of the practical need to compute larger deformations accurately, is *geometrically exact beam and rod theory*, which represents finite rotations and avoids linearization by using rotation tensors, quaternions, or director frames (Reissner 1973, 1981; Simo 1985; Simo and Vu-Quoc 1986, 1991; Antman 2005). These models reduce the three-dimensional continuum to a one-dimensional centerline $\mathbf{a}(s) \in \mathbb{R}^3$ with director triads [columns of $\mathbf{\Theta}(s) \in \mathrm{SO}(3)$] and employ the forms:

$$\mathbf{\Theta}^T\mathbf{\Theta}' \quad \text{and} \quad \mathbf{\Theta}^T\mathbf{a}'$$

to retain fully nonlinear deformation. These two forms are the intrinsic rotation and translation of each rod cross-section expressed in the moving material frame. These two forms, if combined together into one structure, effectively become the left-trivialized derivatives in the special Euclidean algebra $\mathfrak{se}(3)$:

$$\mathbf{g}^{-1}\mathbf{g}' \in \mathfrak{se}(3)\,, \tag{1}$$

where

$$\mathbf{g} = \begin{bmatrix} \mathbf{\Theta} & \mathbf{a} \\ 0 & 1 \end{bmatrix},$$

which is the bridge to the fourth class of elasticity formulation.

The fourth class of elasticity formulation is *geometric mechanics*, which represents configurations on Lie groups such as the special Euclidean group SE(3) with strain-like quantities that arise from left-trivialized derivatives $\mathbf{g}^{-1}\mathbf{g}' \in \mathfrak{se}(3)$ (Marsden and Ratiu 1999). These methods now form the basis of structure-preserving computational schemes in robotics and multibody dynamics.

While (1) is seldom called by its name, which is the Maurer–Cartan form (Cartan 1928, Chevalley 1946), its time-differentiated version is widely used in robotics (see, e.g., Chirikjian and Kyatkin 2000, p. 331; Selig 2005, p. 354; Lynch and Park 2017, p. 98) for motion tracking, where it is referred to as the velocity of the object in the instantaneous body frame (Murray *et al.* 1994, p. 71) or the twist (Lynch and Park 2017). The use of SE(3) in mechanics has evolved from robot kinematics (Denavit and Hartenberg 1955; Paul 1981) where transformations were chained together, then to geometric control (Brockett 1990; Park and Brockett 1994) where velocity began to be seen as an element of a Lie algebra, and then to variational Lie-group mechanics (Marsden and Ratiu 1999) where Lie algebra variables became primary objects. Ideas in the fields of robotics and elasticity then merged, and Lie groups such as SE(3) were adopted into geometrically exact rod formulations where left-trivialized derivatives $\mathbf{g}^{-1}\mathbf{g}' \in \mathfrak{se}(3)$ served as intrinsic kinematic strain measures. A "geometrically exact" Cosserat rod model is one that represents arbitrary bending, twisting, and extension by evolving the rod's configuration on the Lie group SE(3) (position and orientation) and using directors or quaternions to parameterize cross-section orientation at each section location to represent orientation on SO(3) exactly.

Whereas Simo and Vu-Quoc (1986) may have been the first to employ the exponential map for finite rotation updates in geometrically exact nonlinear beam formulations, their formulation remained centered on reconstructing finite rotations from rotation parameters. In contrast, Sonneville *et al.* (2014) formulated the beam configuration directly as an SE(3)-valued field ($\mathbf{g}(s)$), defined the strain as the left-trivialized Maurer–Cartan form given in (1), and derived the discrete equilibrium equations from an energy-based variational principle. This Lie-group formulation yields a structure-preserving discretization that avoids shear and membrane locking while remaining valid for large rotations and finite strains. Locking is a situation where a numerical model becomes artificially stiffer than the actual continuum it is trying to model, thereby causing deflections and strains to be too small, loads to be too large, and convergence to be too slow. Sonneville *et al.* avoided locking because their geometry was never flattened, and SE(3) was never linearized—strain existed in the Lie algebra exactly. Locking is a symptom of a mismatch between the configuration and the strain, so it is avoided by preserving the group structure during discretization. Consequently, most SE(3) formulations do not suffer from classical locking phenomena the way that Timoshenko-type FEM does. Subsequent numerical SE(3)-based studies of geometrically exact Cosserat rods have simulated large bending, large torsion (Surmont and Coache 2020), buckling, looping, and post-buckling configurations using full nonlinear forms (see, e.g., Weeger *et al.* 2017; Till *et al.* 2019; Hante *et al.* 2021; Harsch *et al.* 2023). In these approaches, strain is defined as a Lie-algebra-valued quantity independent of the spatial position within the cross-section, so numerical interpolation is constructed directly on the Lie group rather than interpolating translations and rotations separately. Xun and Tamadazte (2026) presented a Lie-group-consistent Cosserat formulation and a discrete implementation of geometrically exact Cosserat rods subject to torsion, bending, and shear.

The difference between the way the above studies employed the Maurer–Cartan form $\boldsymbol{\xi} = \mathbf{X}^{-1}\partial_x\mathbf{X}$ in describing strain $\boldsymbol{\xi}$ and the present work is that past works have worked with a 1D rod, so their Maurer–Cartan object was pulled back to a curve. In the present study, the Maurer–Cartan form is written $\xi_{kji} = (\mathbf{X}^{-1}\partial_i\mathbf{X})_{kj}$ for multiple spatial directions i, so ξ_{kji} is intended to live on a continuum domain, and the Maurer–Cartan form is elevated from a 1D rod strain measure to a multi-directional continuum strain field satisfying the full Maurer–Cartan compatibility equation.

Another difference with the present work is that in all the past approaches discussed, constitutive laws were formulated in terms of locally defined strain measures such as $\boldsymbol{\xi}$, while geometric information associated with the cross-section was introduced separately through integration, producing quantities such as area moments and torsional constants. Strain at a material point was defined independently of the spatial position of the point within the cross-section. Geometry entered only after the constitutive law through post-processing integrals that generated sectional properties.

In the present work, however, the following affine strain measure will be introduced

$$\boldsymbol{\eta}_i = \boldsymbol{\xi}\cdot\mathbf{R} = \boldsymbol{\Gamma}_{,i}\cdot\mathbf{R} + \boldsymbol{\epsilon}_{,i}$$

that embeds the cross-sectional position $\mathbf{R}$ directly into the strain field. This couples Lie-algebraic deformation measures with intrinsic spatial structure at the constitutive level, allowing sectional geometry to emerge through the strain field itself rather than being

introduced externally. This will allow translational and rotational modes to be unified into a single constitutive relation.

1.2. Non-locality

While the summing of moments might be viewed as more general than the summing of forces since moments can be taken from infinitely far away so that all moment arms drop out, leaving only a sum of forces, the moment itself is not a tensor because $\mathbf{r}\times\mathbf{F}$ does not obey a point transformation. This is because, much like second spatial derivatives, which require the use of Christoffel symbols, the moment is defined between two points, not at a single point. Therefore, the *moment and the angular momentum are not tensors.* The presence of moment arms in a formulation causes it to be non-local and therefore immediately complicates the transformations that can be done on it.

The idea of the *wrench* goes back to Ball (1900) and even Cayley (1869). It is composed of a force and a moment $(\mathbf{M},\mathbf{F})$ and is now mentioned extensively in robotics texts (Murray *et al.* 1994, p. 61; Selig 2005; Lynch and Park 2017, p. 108). The trouble with the wrench is that not only is it non-local, but it is also plagued by the fact that the force and its moment have different units. So while the force and the moment have been unified in one sense for over a century through screw theory (as a 1×6 vector) because basic addition and subtraction of elements and certain other minimal operations could be done with wrenches, the full suite of mathematics could not operate on the wrench as a whole until the work of Denavit and Hartenberg (1955) who used the homogeneous transformation structure that later became standard in robotics; also pivotal was the work of Paul (1981), the first ever use of the exponential map in geometrically exact beam theory by Simo and Vu-Quoc (1986), and the rigorous derivation of the SE(3) exponential map by Park and Brockett (1994). In Cosserat rod theory, the wrench is now unified kinematically and statically, but not constitutively. The wrench is $(\mathbf{M},\mathbf{F})\in\mathfrak{se}(3)$, but when it is related to strain, its force and moment are always treated separately. The force part is governed by EA or GA (where E is Young's modulus; A is area; and G is the shear modulus), and the moment part is governed by EI or GJ (where I and J are the moment of inertia and polar moment of inertia). So while the wrench has been unified in one sense, no constitutive law has unified them until the present work.

Even after the above landmark achievements, some problems related to moment arms still persist, especially in the field of elasticity. For example, the physical component of torsional strain is computed by multiplying the torsional strain (with units of radians/m) by its distance r from the axis of rotation (see, e.g., Gere and Timoshenko 1990). To illustrate how some moment arms can be avoided, a new definition of torque will be given below. When combined with mathematical tools constructed in robotics to transform spatial objects in a metrically proper way, it will allow us to remove some moment arms and appropriately treat those that remain.

An alternate definition of torque that removes the moment arm is the gradient of rotational energy with respect to angle $M=\partial E/\partial\theta$, a relation first proposed by Castigliano (1879) as a theorem. To demonstrate an interesting generalization of it, note that:

$$\mathbf{M} = \frac{\partial E}{\partial\theta} = \frac{\mathrm{d}E}{\mathrm{d}\theta} = \frac{\mathrm{d}(\mathbf{F}\mathrm{d}\mathbf{s})}{\mathrm{d}\theta} = \frac{\mathbf{F}(\mathbf{e}_1 r_1)(\mathbf{e}_1\mathbf{e}_2\mathrm{d}\theta)}{\mathrm{d}\theta} = \frac{\mathbf{e}_1 F(\mathbf{e}_1 r_1)(\boldsymbol{i}\mathrm{d}\theta)}{\mathrm{d}\theta} = \boldsymbol{i}F\,r\,,$$

where $\mathbf{e}_1$ and $\mathbf{e}_2$ are basis vectors, and $\boldsymbol{i} = \sqrt{-1} = \mathbf{e}_1\,\mathbf{e}_2$ because $\mathbf{e}_1\,\mathbf{e}_2 = -\mathbf{e}_2\,\mathbf{e}_1$. One could argue that the moment arm still appears, but something different has happened here. The material was given a say in what the moment arm is. When torque is applied to a body as an external boundary condition, use of the moment arm is explicit and proper. However, the moment arm appearing above is different because it was selected by the material itself based on its geometry. The same thing happens when we throw a hammer—we apply the force and the torque, but the hammer decides where to put its own axis of rotation. The moment arm that arises within the material is indistinguishable from the metric component, $\sqrt{g_{22}}$ say, that is used to convert a tensor component such as θ, into a physical component of velocity v.

Let us generalize the above demonstration slightly, keeping careful track of the basis vectors:

$$\frac{\partial E}{\partial \boldsymbol{\theta}} = \frac{\partial E}{\partial(\boldsymbol{i}\theta)} = \frac{\sum_{i,k}\mathbf{e}_i F_i\,\partial\mathbf{s}_k}{\mathbf{e}_1\,\mathbf{e}_2\,\partial\theta} = \frac{\mathbf{e}_1 F_1\,\partial\mathbf{s}_1 + \mathbf{e}_2 F_2\,\partial\mathbf{s}_2 + \mathbf{e}_1 F_1\,\partial\mathbf{s}_2 + \mathbf{e}_2 F_2\,\partial\mathbf{s}_1}{\mathbf{e}_1\,\mathbf{e}_2\,\partial\theta}$$

Writing $\partial\mathbf{s}_1 = \partial(\mathbf{e}_2 r_2\,\mathbf{e}_1\mathbf{e}_2\theta)$ and $\partial\mathbf{s}_2 = \partial(\mathbf{e}_1 r_1\,\mathbf{e}_1\mathbf{e}_2\theta)$, we get

$$\begin{aligned}
\frac{\partial E}{\partial \boldsymbol{\theta}} &= \frac{\mathbf{e}_2\,\mathbf{e}_1\,[\mathbf{e}_1 F_1\,\partial(\mathbf{e}_2 r_2\,\mathbf{e}_1\mathbf{e}_2\theta) + \mathbf{e}_2 F_2\,\partial(\mathbf{e}_1 r_1\,\mathbf{e}_1\mathbf{e}_2\theta) + \mathbf{e}_1 F_1\,\partial(\mathbf{e}_1 r_1\,\mathbf{e}_1\mathbf{e}_2\theta) + \mathbf{e}_2 F_2\,\partial(\mathbf{e}_2 r_2\,\mathbf{e}_1\mathbf{e}_2\theta)]}{\partial\theta} \\
&= \frac{\mathbf{e}_2\,\mathbf{e}_1\,[-\mathbf{e}_1 F_1\,\mathbf{e}_1 r_2\,\partial\theta + \mathbf{e}_2 F_2\,\mathbf{e}_2\,r_1\,\partial\theta + \mathbf{e}_1 F_1\,\mathbf{e}_2\,r_1\,\partial\theta + F_2\,\mathbf{e}_1\mathbf{e}_2\,r_2\,\partial\theta]}{\partial\theta} \\
&= \frac{(\mathbf{e}_1\,\mathbf{e}_2\,F_1\,r_2 - \mathbf{e}_1\,\mathbf{e}_2\,F_2\,r_1 + F_1\,r_1 + F_2\,r_2)\partial\theta}{\partial\theta} \\
&= \mathbf{e}_1\,\mathbf{e}_2(r_2 F_1 \;-\; r_1 F_2) \;+\; F_1 r_1 \;+\; F_2 r_2
\end{aligned}$$

If $\mathbf{F} = m\boldsymbol{g}$, then the relation for the partial derivative of energy with respect to angle becomes

$$\frac{\partial E}{\partial \boldsymbol{\theta}} = \mathbf{M} \;+\; m\mathbf{g}\cdot\mathbf{h}\,. \tag{2}$$

The far right term is potential energy, a fact that brings to mind the Helmholtz decomposition theorem, which states that any continuous vector can be decomposed into the gradient of a scalar potential and the curl of a vector potential. And for a shaft in pure torsion and only axial compression, the torsion does, in fact, correspond to a vector potential within the material, but when more complex loads are applied, the utility of Helmholtz's theorem diminishes. Of course everything hinges on what d$\mathbf{s}$ was. If it was displacement, then the formulation gives strain energy; if d$\mathbf{s}$ was merely a distance, then the relation gives a potential. Whether or not this potential can be construed as potential (extractable) energy depends on the neighboring material around the point in question. Alternatively, energy-like and moment-like quantities may be components of a single multivector potential. They may be different grade components of the same geometric entity. The concept in (2) will be used to formulate a constitutive relation for the wrench, which contains both force and moment. The interesting aspect of (2) is that a single geometric generating object can produce physically distinct quantities through grade selection. We will see something similar in Example 3 of §2.4.5, where torsion and bending arise through different grades of a moment flux object $\boldsymbol{\mu}$. Another important aspect of (2) is that we obtained torque not by including a moment arm, but by peeling off, or factoring out, curvature.

1.3. Main contributions

The word "intrinsic" as used here means that a relation is independent of the choice of coordinates. For example, the Euler-Lagrange equation would be considered intrinsic even when it is written in coordinate form because it takes the same algebraic form when written in any other coordinate system. Formulations that are not intrinsic are those whose constitutive law depends on the chosen sectional axes, precomputed section properties such as I_1, I_2, or J, or decomposition into separate bending, torsion, and shear modes.

The present formulation employs the SE(3) configuration space and Maurer–Cartan strain of geometrically exact Cosserat rod theory and so accommodates finite rotations and translations. However, in the present work, the intrinsic Maurer–Cartan strain generator $\boldsymbol{\xi}_i = \mathbf{X}^{-1}\partial_i\mathbf{X}$ is multidimensional, and the strain measure $\boldsymbol{\eta}$ is not identified directly with the Lie algebra element. Instead, as discussed earlier, an affine contraction map couples the Lie-algebraic strain $\boldsymbol{\xi}$ to an intrinsic cross-sectional position field $\mathbf{R}$, producing a derived strain quantity $\boldsymbol{\eta}$ that embeds geometric information at the constitutive level.

Two aspects of the present formulation are intrinsic. First, the strain generator $\boldsymbol{\xi}$ obtained by the Maurer–Cartan form depends only on local deformation and not on the body's absolute placement in space. Second, the material property matrix $\mathbf{K}$ includes only intrinsic material properties E and G. Classical sectional stiffnesses such as EA, EI, and GJ are not prescribed constitutive parameters. Instead, they emerge through spatial integration of the affine strain field and therefore appear as derived geometric invariants rather than inputs to the constitutive law. As a result, classical axial, bending, and torsional stiffnesses emerge naturally from the induced strain field rather than by being introduced as independent constitutive parameters. Torsional warping and bending shear arise as compatibility consequences of the affine SE(3) structure rather than as independently introduced auxiliary fields.

Whereas stresses within cross sections are often approximated through assumed distributions, the present formulation employs a single affine constitutive relation together with a unified wrench expression that provides an explicit analytical relation between external boundary conditions and internal stress fields throughout bodies under combined bending, torsion, and axial loading.

Because the solutions are explicit, they can be coupled with spreadsheet solvers or optimization tools to quickly optimize for stress-minimizing geometries. The theory reproduces classical bending, torsion, and axial stress relations while retaining finite-rotation SE(3) kinematics.

2. Intrinsic SE(3) Elasticity

2.1. Representing Position and Orientation Together (Configuration)

The configuration of a body will be denoted, as it is in robotics (Brockett 1990), by

$$\mathbf{X}(x,t) \;=\; \begin{bmatrix} \boldsymbol{\Theta} & \mathbf{a} \\ 0 & 1 \end{bmatrix}. \tag{3}$$

Here, $\boldsymbol{\Theta}$ is a 3×3 rotation matrix, and $\mathbf{a}\in\mathbb{R}^3$ is the translational position of the local frame in the reconstructed SE(3) configuration field, so $\mathbf{X}$ is a member of the special Euclidean

group SE(3), which consists of all rigid body motion. This configuration $\mathbf{X}$ configures, or processes, points $\mathbf{r}$ in space, as follows:

$$\mathbf{r}_2 = \mathbf{X}\mathbf{r}\,, \tag{4}$$

$$\mathbf{r}_2 = \mathbf{\Theta}\mathbf{r} + \mathbf{a}\,.$$

But since the subscript "2" could be misunderstood hereafter as the y-component of $\mathbf{r}$, the second point $\mathbf{r}_2$ will be simply called $\mathbf{p}$ rather than $\mathbf{r}_2$. Therefore,

$$\mathbf{p} = \mathbf{\Theta}\mathbf{r} + \mathbf{a}\,. \tag{5}$$

Rotational and translational strain are combined into one transformation $\mathbf{X} = \mathbf{\Theta} + \mathbf{a}$, and the $\mathbf{r}$'s are written in homogeneous coordinates, i.e.,

$$\mathbf{r} = \begin{bmatrix} x \\ y \\ z \\ 1 \end{bmatrix}.$$

A new point in space is located by the affine transformation in (5) where $\mathbf{r}$ gets rotated by $\mathbf{\Theta}\mathbf{r}$ and translated by $\mathbf{a}$. Then, since $\Delta\mathbf{r} = \mathbf{p} - \mathbf{r}$, we can write

$$\Delta\mathbf{r} = \mathbf{\Theta}\mathbf{r} + \mathbf{a} - \mathbf{r}\,. \tag{6}$$

Grouping terms with $\mathbf{r}$ and renaming $\Delta\mathbf{r}$ as $\boldsymbol{\zeta}$ gives

$$\boldsymbol{\zeta} = (\mathbf{\Theta} - \mathbf{I})\mathbf{r} + \mathbf{a} \tag{7}$$

or

$$\boldsymbol{\zeta} = \mathbf{X}\mathbf{r} - \mathbf{r}\,. \tag{8}$$

The matrix $\mathbf{\Theta}$ and the vector $\mathbf{a}$ have different units, but this is allowable because they occupy different spaces in the matrix $\mathbf{X}$. And this units mismatch will turn out to be a benefit when formulating a method that calculates both moment and force with a single formula.

It is important to note that the Δ appearing in (6) is not an approximation that will later need to be shrunk to a small limit in order to be valid. The beauty of the structure is that it is exact.

2.2. Intrinsic Differential Kinematics (Motion)

For a quick review of the relevant mathematics from robotics, the components of motion are written as shown on the left side of (9) and, in some engineering contexts, are written as shown on the right side of (9):

$$\mathbf{V} = \mathbf{X}^{-1}\partial_t\mathbf{X} = \begin{bmatrix} \dot{\boldsymbol{\theta}} & \dot{\mathbf{a}} \\ 0 & 0 \end{bmatrix} \qquad \mathbf{V} = \begin{bmatrix} \dot{\theta}_x \\ \dot{\theta}_y \\ \dot{\theta}_z \\ v_x \\ v_y \\ v_z \end{bmatrix} \quad \text{(body motion)} \tag{9}$$

The form on the left is the Maurer–Cartan form (Cartan 1904, 1928; Chevalley 1946), but in robotics, it is usually called a twist (Murray and Sastry 1990).

To confirm (9), write the group element

$$\mathbf{X}(z,t) \;=\; \begin{bmatrix} \mathbf{\Theta}(\theta(z,t)) & \mathbf{a}(z,t) \\ 0 & 1 \end{bmatrix}$$

and its inverse

$$\mathbf{X}^{-1} \;=\; \begin{bmatrix} \mathbf{\Theta}^{-1} & -\mathbf{\Theta}^{-1}\mathbf{a} \\ 0 & 1 \end{bmatrix},$$

and take the time derivative:

$$\frac{\partial \mathbf{X}}{\partial t} \;=\; \begin{bmatrix} \dot{\mathbf{\Theta}} & \dot{\mathbf{a}} \\ 0 & 1 \end{bmatrix}. \tag{10}$$

Then the motion $\mathbf{V}$ is given by (9):

$$\mathbf{V} \;=\; \mathbf{X}^{-1}\frac{\partial \mathbf{X}}{\partial t} \;=\; \begin{bmatrix} \mathbf{\Theta}^{-1}\dot{\mathbf{\Theta}} & \mathbf{\Theta}^{-1}\dot{\mathbf{a}} \\ 0 & 0 \end{bmatrix}. \tag{11}$$

Here, we see that the rotation part is

$$\mathbf{\Theta}^{-1}\dot{\mathbf{\Theta}} \;=\; \dot{\theta}\,\mathbf{B} \;=\; \mathbf{\Omega}\,, \tag{12}$$

where $\mathbf{B}$ is the generator (a skew matrix or bivector), and $\dot{\theta}$ is the magnitude.

The translation part is

$$\mathbf{v} \;=\; \mathbf{\Theta}^{-1}\,\dot{\mathbf{a}} \;\approx\; \dot{\mathbf{a}}\,, \tag{13}$$

which happens to be $\dot{\mathbf{a}}$ for small rotations.

In light of (13) and (12), we can say that $\mathbf{V}$ in (11) is

$$\mathbf{V} \;=\; \begin{bmatrix} \mathbf{\Omega} & \mathbf{v} \\ 0 & 0 \end{bmatrix}. \tag{14}$$

The velocity $\mathbf{V}$ naturally lives in an algebra, but only if it is formulated as on *the left side of* (9). The 1×6 vectors on the right side are merely vectors. They can be scaled, and like components can be added together; however, we cannot multiply two of them together to get a third. Therefore, the 1×6 vectors are not elements of an algebra. The vector multiplication that the 1×6 vectors are missing is the Lie bracket (what 3D vectors allow the cross product to imitate):

$$[\mathbf{A},\mathbf{B}] \;=\; \mathbf{A}\,\mathbf{B} \;-\; \mathbf{B}\,\mathbf{A}\,,$$

which appropriately describes the non-commutativity of large consecutive rotations about different axes. It is this property of matrix multiplication that naturally handles rotational geometry, including commutators, exponential maps, and finite rotations. The 4×4 representation of Denavit and Hartenberg (1955) gives us direct connection to SE(3). None of the extra benefits of the Lie-algebra structure are available to 1×6 vectors. The flattening of the matrices into 1×6 vectors breaks the Lie-algebraic structure of SE(3). The flattened 1×6 "stress" vector does not transform under rotations the way ordinary stress tensors do.

The 1×6 notation was introduced by Voigt (1910) to reduce the number of elements of the stress and strain tensors from 9 to 6 by exploiting the assumption that the stress tensor

is symmetric. This then required 3 elements for the diagonals and only 3 distinct off-diagonal elements. This reduced the complexity and made the material stiffness matrix more comprehensible, reducing it from a rank 4 tensor to a rank 2 tensor (see, e.g., Boresi and Schmidt 2003, Chapter 3). As Mánik (2021) noted most succinctly, one of the main practical problems with flattening the stress tensor into a 1×6 vector is that $\boldsymbol{\sigma}:\boldsymbol{\sigma} \neq (\boldsymbol{\sigma}^{\mathrm{V}})^T\boldsymbol{\sigma}^{\mathrm{V}}$ (the superscript "^{V}" denotes the operation of "vectorizing" the stress tensor into a 1×6 vector). To remedy this problem, Mandel (1965) proposed incorporating a weighting of $\sqrt{2}$ with the shear components, as follows: $\boldsymbol{\sigma}^M = [\sigma_{11}, \sigma_{22}, \sigma_{33}, \sqrt{2}\sigma_{23}, \sqrt{2}\sigma_{13}, \sqrt{2}\sigma_{12}]$. An in-depth study on this issue was conducted by Helnwein (2001), who showed, among other things, that an orthonormal basis for tensor representation in $\mathbb{R}^3$ does not automatically lead to a normalized space for the flattened matrix representation in $\mathbb{R}^6$. Mathematically at least, the 1×6 stress vectors can represent a metric space because this can be done by simply equipping the space with an appropriate inner product (or metric). However, the Euclidean metric so created will not be the physically appropriate one. The physical norm created by symmetric tensors $\boldsymbol{\alpha}$ and $\boldsymbol{\beta}$ that are in two spaces dual to each other is: $\left\langle \boldsymbol{\alpha}, \boldsymbol{\beta} \right\rangle = \alpha_{ik}\,\beta_{ik}$, without extraneous weightings. For more on why Lie groups are central in mechanics, see Bloch (2015).

2.3. Intrinsic Strain

The present elasticity formulation will utilize the same form as (3), and $\mathbf{X}$ will still be an affine configuration field. Two processes can change the configuration of a body: the passage of time and deformation of the material. How this configuration $\mathbf{X}$ changes with time becomes the kinematics. How the configuration changes spatially will become elasticity, provided those deformations are weighted by the material resistances appropriate to their respective modes of deformation (G and E).

Recall that the classical strain definition

$$\epsilon_{ij}^{\text{class.}} = \frac{1}{2}\left(\frac{\partial u_i}{\partial x_j} + \frac{\partial u_j}{\partial x_i}\right) \qquad \text{(approximate strain)} \tag{15}$$

is approximate. In the present work, the same variable name ϵ will be used hereafter, but the definition in (15) will not be assigned to it. Instead, an exact definition will be given.

The Maurer–Cartan form can be viewed as two separate forms. The temporal Maurer–Cartan form

$$\boldsymbol{\xi}_{,t} = \mathbf{X}^{-1}\partial_t\mathbf{X} \qquad \text{(kinematics, robotics)}$$

describes body velocity, angular velocity, and rigid-body dynamics; whereas the spatial Maurer–Cartan form

$$\boldsymbol{\xi}_{,z} = \mathbf{X}^{-1}\partial_z\mathbf{X} \qquad \text{(strain, elasticity)}$$

can describe the strain gradient as has been done in the past. That is, components of strain could be given by the same Maurer–Cartan form

$$\boldsymbol{\xi} = \mathbf{X}^{-1}\partial_z\mathbf{X}$$

so that

$$\boldsymbol{\xi} = \begin{bmatrix} \boldsymbol{\Gamma} & \boldsymbol{\epsilon} \\ 0 & 0 \end{bmatrix},$$

where $\boldsymbol{\Gamma}$ and $\boldsymbol{\epsilon}$ would be the rotational and translational strain gradients, respectively. However, the standard SE(3) translational part ϵ_k is only a vector. It gives one column at a time. There is no object ϵ_{ki} with two indices inside ordinary SE(3). This presents a problem when we attempt to formulate a constitutive relation between the energy density w and any strain measure. To compute stresses for shear, bending, torsion, *etc.*, we need all 9 components of the strain tensor, not merely a single column. Therefore ϵ_k will be promoted to $\epsilon_{k,i}$, which will be a full translational strain-gradient tensor. Then, strain becomes

$$\boldsymbol{\xi}_i = \begin{bmatrix} \boldsymbol{\Gamma}_{,i} & \boldsymbol{\epsilon}_{,i} \\ 0 & 0 \end{bmatrix}, \tag{16}$$

and is a 4×4 matrix for each direction i. Incidentally, $\boldsymbol{\xi}$ could probably be treated as a Lie-algebra-valued 1-form $\boldsymbol{\xi} = \boldsymbol{\xi}_i \, \mathrm{d}x_i$.

So at this point, we leave pure SE(3) because the translational part of $\mathfrak{se}(3)$ is $\mathbb{R}^3$, not $\mathbb{R}^{3\times 3}$. In other words, $\epsilon_{k,i} \notin \mathfrak{se}(3)$. But even though the resulting $\boldsymbol{\xi}$ cannot be viewed as a genuine SE(3) strain, we can modify our interpretation slightly and view (16) as a bundle of directional generators. Each column $\boldsymbol{\epsilon}_{,i}$ is still an SE(3)-type translational generator. Thus the theory will retain SE(3)-based kinematics, but the constitutive distortion space will be larger than $\mathfrak{se}(3)$ because $\boldsymbol{\epsilon}$ is a full matrix rather than a Lie-algebra translation vector. Each directional strain generator $\boldsymbol{\xi}_i$ will act affinely on a given cross-sectional position.

In index notation, the spatial derivative in the Maurer–Cartan form to be used is

$$\xi_{kji} = (\mathbf{X}^{-1}\partial_i \mathbf{X})_{kj} \qquad \text{(strain, exact)} \tag{17}$$

The inverse $\mathbf{X}^{-1}$ will be of the form

$$\mathbf{X}^{-1} = \begin{bmatrix} \mathbf{A} & \mathbf{b} \\ 0 & 1 \end{bmatrix}$$

such that $\mathbf{X}^{-1}\mathbf{X} = \mathbf{I}$. To find it, multiply

$$\begin{bmatrix} \mathbf{A} & \mathbf{b} \\ 0 & 1 \end{bmatrix}\begin{bmatrix} \boldsymbol{\Theta} & \mathbf{a} \\ 0 & 1 \end{bmatrix} = \begin{bmatrix} \mathbf{A}\boldsymbol{\Theta} & \mathbf{A}\mathbf{a}+\mathbf{b} \\ 0 & 1 \end{bmatrix},$$

and set it equal to $\mathbf{I}$

$$\begin{bmatrix} \mathbf{I} & 0 \\ 0 & 1 \end{bmatrix}$$

to find that

$$\mathbf{A} = \boldsymbol{\Theta}^{-1} \qquad \text{and} \qquad \mathbf{b}\boldsymbol{\Theta}^{-1} + \mathbf{a} = 0\,.$$

Therefore, the inverse of $\mathbf{X}$ is

$$\mathbf{X}^{-1} = \begin{bmatrix} \boldsymbol{\Theta}^{-1} & -\boldsymbol{\Theta}^{-1}\mathbf{a} \\ 0 & 1 \end{bmatrix}.$$

To compute $\boldsymbol{\xi}$ in (17), multiply $\mathbf{X}^{-1}$ by $\partial_i \mathbf{X}$:

$$\boldsymbol{\xi}_i = \begin{bmatrix} \boldsymbol{\Theta}^{-1} & -\boldsymbol{\Theta}^{-1}\mathbf{a} \\ 0 & 1 \end{bmatrix}\begin{bmatrix} \partial_i\boldsymbol{\Theta} & \partial_i\mathbf{a} \\ 0 & 0 \end{bmatrix}.$$

So the strain gradient is

$$\boldsymbol{\xi}_i = \mathbf{X}^{-1}\frac{\partial \mathbf{X}}{\partial x_i} = \begin{bmatrix} \boldsymbol{\Theta}^{-1}\partial_i\boldsymbol{\Theta} & \boldsymbol{\Theta}^{-1}\partial_i\mathbf{a} \\ 0 & 0 \end{bmatrix}. \tag{18}$$

The multiplication on the left by the inverse of $\mathbf{X}$ is what makes the Maurer–Cartan form intrinsic. The mere gradient $\partial_i\mathbf{X}$ is not a Lie-algebra element, so it cannot be directly compared at different configurations. But the Maurer–Cartan form above transports everything back to the identity so that $\boldsymbol{\xi} \in \mathfrak{se}(3)$ for every configuration. This produces a space for common comparison.

Decomposing (18), we can see that

$$\boldsymbol{\xi}_i = \underbrace{\boldsymbol{\Theta}^{-1}\partial_i\boldsymbol{\Theta}}_{\substack{\text{rotational}\\ \text{strain}}} + \underbrace{\boldsymbol{\Theta}^{-1}\partial_i\mathbf{a}}_{\substack{\text{translational}\\ \text{strain}}} \tag{19}$$

So write

$$\boldsymbol{\xi}_i = \begin{bmatrix} \boldsymbol{\Gamma}_{,i} & \boldsymbol{\epsilon}_{,i} \\ 0 & 0 \end{bmatrix} \qquad \text{(exact strain)} \tag{20}$$

so that

$$\boldsymbol{\Gamma}_{,i} = \boldsymbol{\Theta}^{-1}\frac{\partial \boldsymbol{\Theta}}{\partial x_i} \tag{21}$$

and

$$\boldsymbol{\epsilon}_{,i} = \boldsymbol{\Theta}^{-1}\frac{\partial \mathbf{a}}{\partial x_i} \tag{22}$$

are the rotational and translational strain gradients, respectively. The rotational strain matrix $\boldsymbol{\Gamma}$ is skew-symmetric and has units of 1/m, and the translational strain gradient $\boldsymbol{\epsilon}$ is dimensionless. The unit mismatch in (20) will be essential in constructing a unified formula for the force and moment contained in the wrench. This formulation is powerful and will provide exact displacements for large deformations using the exponential map. The exact form of strain in (22) obtained from the SE(3) formulation is therefore superior to (15) because it tells what the deformation means in the current material frame. After all, a partial derivative such as that in (15) is part of a Taylor series extrapolation to a nearby point—an inherent approximation. The dimensionless local deformation may be written $\mathrm{d}\zeta_k/\mathrm{d}x_i = u_{k,i}$, where $\boldsymbol{\zeta}$ was defined in (7); however, $u_{k,i}$, or $\epsilon_{ki}^{\text{class.}}$, is not generally identical to $\epsilon_{k,i}$ because $\epsilon_{k,i}$ is only the translational part of the intrinsic SE(3) strain. The rotational contribution enters through $\boldsymbol{\Gamma}_i \cdot \mathbf{R}$. The total intrinsic strain measure preserves directional information that is discarded when the classical symmetric strain tensor is formed.

Now suppose, for example, that we have a circular shaft in pure torsion about the z axis. The angle of twist $\phi(z)$ of a section plane is at most a function of z. Then

$$\boldsymbol{\Theta} = \begin{bmatrix} \cos\phi(z) & -\sin\phi(z) & 0 \\ \sin\phi(z) & \cos\phi(z) & 0 \\ 0 & 0 & 1 \end{bmatrix}, \tag{23}$$

and in this case the point map is, from (4), simply

$$\mathbf{r}_2 = \mathbf{\Theta}(z)\mathbf{r}$$

$$\mathbf{r}_2 = \begin{bmatrix} x_2 \\ y_2 \\ z_2 \end{bmatrix} = \begin{bmatrix} x\cos\phi - y\sin\phi \\ x\sin\phi + y\cos\phi \\ z \end{bmatrix} \tag{24}$$

Computing the two matrices on the right side of (21) gives

$$\mathbf{\Gamma}_{,z} = \begin{bmatrix} \cos\phi(z) & \sin\phi(z) & 0 \\ -\sin\phi(z) & \cos\phi(z) & 0 \\ 0 & 0 & 1 \end{bmatrix} \begin{bmatrix} -\phi'\sin\phi(z) & -\phi'\cos\phi(z) & 0 \\ \phi'\cos\phi(z) & -\phi'\sin\phi(z) & 0 \\ 0 & 0 & 0 \end{bmatrix}.$$

Multiplying, we find that

$$\mathbf{\Gamma}_{,z} = \phi' \begin{bmatrix} 0 & -1 & 0 \\ 1 & 0 & 0 \\ 0 & 0 & 0 \end{bmatrix} = \phi'\mathbf{G}_z\,. \tag{25}$$

So contrary to appearances, no small-angle approximation has been made.

In summary, the configuration $\mathbf{X}$ given in (3) contains finite configuration variables (elements of a group), and $\boldsymbol{\xi}$ and $\mathbf{V}$ contain infinitesimal generators (elements of an algebra). The configuration (3) represents a change in the pose (the position and orientation) of a body, so $\mathbf{V} = \mathbf{X}^{-1}\mathrm{d}\mathbf{X}$ would tell us the instantaneous infinitesimal motion generating the evolution. Repeated multiplication by $\mathbf{X}$ tells where the body is but not its internal strain. The gradient matrix $\boldsymbol{\xi}$ defined by the spatial Maurer–Cartan form is the infinitesimal generator of SE(3) transformations that gives the local rotational and translational strain gradients.

The beauty of (17) is that we can integrate it as a differential equation for $\mathbf{X}$. First, multiply it by $\mathbf{X}$:

$$\frac{\mathrm{d}\mathbf{X}}{\mathrm{d}z} = \mathbf{X}\boldsymbol{\xi}\,. \tag{26}$$

Then substitute in the matrices on the right sides using (3) and (20), and obtain

$$\frac{\mathrm{d}\mathbf{X}}{\mathrm{d}z} = \begin{bmatrix} \mathbf{\Theta} & \mathbf{a} \\ 0 & 1 \end{bmatrix} \begin{bmatrix} \mathbf{\Gamma} & \boldsymbol{\epsilon} \\ 0 & 0 \end{bmatrix}$$

$$\frac{\mathrm{d}\mathbf{X}}{\mathrm{d}z} = \begin{bmatrix} \mathbf{\Theta\Gamma} & \mathbf{\Theta}\boldsymbol{\epsilon} \\ 0 & 1 \end{bmatrix} \tag{27}$$

Noting how $\mathbf{X}$ is defined in (3) allows us to solve the rotational and translational parts separately. First, by comparing the top left 3×3 matrices, we have

$$\frac{\mathrm{d}\mathbf{\Theta}}{\mathrm{d}z} = \mathbf{\Theta\Gamma}\,. \tag{28}$$

Integrating gives the exact rotation field (how the plane at z is rotated due to strain):

$$\mathbf{\Theta}(z) = \mathbf{\Theta}(0)\,e^{\int_0^z \mathbf{\Gamma}\mathrm{d}z}\,, \tag{29}$$

where $\mathbf{\Theta}(0) = \mathbf{I}$. As the integration here shows, variation of $\mathbf{\Gamma}$ with z is easily accommodated.

Next, by comparing the top right entries of (27) and (3), we find that

$$\frac{\mathrm{d}\mathbf{u}}{\mathrm{d}z} = \mathbf{\Theta}\,\boldsymbol{\epsilon}_{,z} \tag{30}$$

Integrating gives the exact translational component of the configuration field:

$$\mathbf{a}(z) = \int_0^z \mathbf{\Theta}(z)\,\boldsymbol{\epsilon}(z)\mathrm{d}z\,. \tag{31}$$

2.3.1 Configuration field along z-axis:

Recall from (4) and (8) that when we write $\mathbf{r}$ in homogeneous coordinates, we have the identities:

$$\mathbf{r}_2 = \mathbf{X}\,\mathbf{r} \qquad \text{and} \qquad \Delta\mathbf{r} = \mathbf{X}\,\mathbf{r} - \mathbf{r}\,.$$

And $\mathbf{X}(z)$ is the configuration of the cross section at coordinate z. Therefore, $\mathbf{\Theta}(z)$ is the orientation of the entire cross-section at position z. The independent variable is the beam coordinate. In SE(3), the configuration $\mathbf{X}$ of the displaced cross section can be reconstructed from the Maurer–Cartan form along a spatial coordinate such as z. We simply integrate (26) to get the configuration of the body

$$\begin{aligned}\mathbf{X}(z) &= \mathbf{X}(0)\exp\left(\int_0^z \boldsymbol{\xi}_z(s)\mathrm{d}s\right) \\ &= \begin{bmatrix}\mathbf{\Theta} & \mathbf{a} \\ 0 & 1\end{bmatrix},\end{aligned} \tag{32}$$

where the Maurer–Cartan form gives its strain gradient:

$$\boldsymbol{\xi}_{,z}(z) = \mathbf{X}^{-1}\frac{\partial\mathbf{X}}{\partial x_z} = \begin{bmatrix}\mathbf{\Gamma}_{,z} & \boldsymbol{\epsilon}_{,z} \\ 0 & 0\end{bmatrix} \in \mathfrak{se}(3) \tag{33}$$

Here, $\mathbf{\Gamma}_{,z} \in \mathfrak{so}(3)$ is an infinitesimal rotation along z, and $\boldsymbol{\epsilon}_{,z} \in \mathbb{R}^3$ is an infinitesimal translational strain along z.

In robotics, repeated SE(3) multiplication describes finite rigid-body transformations and global kinematics, and the temporal Maurer–Cartan form describes infinitesimal generators. Similarly, the spatial Maurer–Cartan form describes infinitesimal generators such as local strain, torsion, and intrinsic elastic deformation by means of (32), which is the Lie-group analogue of integrating velocity over time to obtain position. The deformed configuration of the body is reconstructed from the local strain field. In each direction i, the configuration satisfies

$$\mathbf{X}_{,i} = \mathbf{X}\,\boldsymbol{\xi}_{,i}$$

In three dimensions, reconstruction along a path therefore proceeds by integrating the appropriate directional equations. The full intrinsic local strain associated with direction i is represented by the 4×4 Lie-algebra matrix

$$\boldsymbol{\xi}_i = \begin{bmatrix}\Gamma_{11,i} & \Gamma_{12,i} & \Gamma_{13,i} & \epsilon_{1,i} \\ \Gamma_{21,i} & \Gamma_{22,i} & \Gamma_{23,i} & \epsilon_{2,i} \\ \Gamma_{31,i} & \Gamma_{32,i} & \Gamma_{33,i} & \epsilon_{3,i} \\ 0 & 0 & 0 & 0\end{bmatrix}.$$

In the same way that velocity, which is in the special Euclidean algebra $\mathfrak{se}(3)$, is a generator of infinitesimal translation along a curve, $\boldsymbol{\Gamma}_i \in \mathfrak{se}(3)$ is a generator of infinitesimal rotational strain along direction i, and $\boldsymbol{\epsilon}_i \in \mathbb{R}^3$ is a generator of infinitesimal translational strain. The exponential map $\exp\colon \mathfrak{se}(3) \to \mathrm{SE}(3)$ reconstructs, along direction i, the finite displacements. Torsion, bending, compression, or any combination of them are described by $\boldsymbol{\xi}$. The exponential map integrates the local infinitesimal strain and rotation into a global configuration. For combined loads, the total rotation matrix $\boldsymbol{\Theta}(z)$ can be written as the product of two rotation matrices—bending denoted by $\boldsymbol{\Theta}_B(z)$ and torsion denoted by $\boldsymbol{\Theta}_T(z)$ as follows:

$$\boldsymbol{\Theta}(z) \;=\; \boldsymbol{\Theta}_T(z)\boldsymbol{\Theta}_B(z)\,.$$

As shown in (28), the rotational evolution is

$$\boldsymbol{\Theta}'(z) \;=\; \boldsymbol{\Theta}(z)\,\boldsymbol{\Gamma}(z)\,.$$

2.4. Mechanics

2.4.1 Energy stored by deformation

In order to recover both moments and forces when integrating over a cross section, the strain energy density w must involve not only translational strain $\boldsymbol{\epsilon}$ as is typically done, but must also depend on the rotationally induced strain gradient $\boldsymbol{\Gamma}_{,i}$. Unlike fluids, solid bodies have structural strength that allows them to transmit forces great distances. Therefore, the constitutive relation must account for this. Accordingly, we apply the Maurer–Cartan strain to the point $\mathbf{R}$:

$$\boldsymbol{\eta}_i \;=\; \boldsymbol{\xi}_{,i}\cdot\mathbf{R}\,. \tag{34}$$

Here, $\mathbf{R}$ is a vector pointing from the centroid $\bar{\mathbf{r}}$ of the domain to the point of interest at $\mathbf{r}$:

$$\mathbf{R} \;=\; \mathbf{r} \;-\; \bar{\mathbf{r}}\,. \tag{35}$$

Therefore, (34) can also be written as

$$\boldsymbol{\eta}_i \;=\; \boldsymbol{\Gamma}_{,i}\cdot\mathbf{R} \;+\; \boldsymbol{\epsilon}_{,i} \tag{36}$$

Notice that this is the same type of affine transformation as in (5). The point $\bar{\mathbf{r}}$ is not guessed but can be shown to emerge from an energy minimization condition. For pure homogeneous bending, minimization of energy shows that $\bar{\mathbf{r}}$ lies on the centroid. The point $\bar{\mathbf{r}}$ is the point about which the section stores the minimum energy. If, instead, the absolute position $\mathbf{r}$ were used in (36), then shifting the origin would change the local stresses thus computed and make them dependent on arbitrary coordinate changes. The relation in (34) is the infinitesimal affine action of the Maurer–Cartan strain generator on a material point. Therefore, $\boldsymbol{\eta}$ is the strain analogue of the velocity field generated by a twist in robotics.

In full index notation, (36) is written

$$\eta_{ki} \;=\; \Gamma_{kj,i}\,R_j \;+\; \epsilon_{k,i}\,, \tag{37}$$

where i is the index generated by taking the gradient, k is the strain or force direction, and j is the local position component within the section.

For every load case examined in this study, the variationally selected point $\bar{\mathbf{r}}$ has been the centroid. Those cases include: pure torsion, pure bending, pure axial compression, pure shear, combined bending and torsion, and combined bending, torsion, and axial compression. The cross-sections examined were rectangular sections and triangular sections. Initially, the point was thought to be the neutral axis because the neutral axis is where bending stress vanishes. The calculations instead suggest that $\bar{\mathbf{r}}$ is tied to elimination of first moments of strain energy, whereas the neutral axis is tied to $\eta_{33} = 0$, which is a different condition. The neutral axis depends on the applied loading, whereas the centroid depends only on geometry. Thus far, the mathematics has consistently selected the geometric quantity, not the loading-dependent one. That suggests that the point $\bar{r}_j$ in $\eta_{ki} = \Gamma_{kj,i}(r_j - \bar{r}_j) + \epsilon_{k,i}$ is fundamentally a geometric center rather than a stress center.

The strain energy w stored in the body is

$$w \;=\; \frac{1}{2}E({\eta_{11}}^2 + {\eta_{22}}^2 + {\eta_{33}}^2) \;+\; \frac{1}{2}G[(\eta_{12}+\eta_{21})^2 + (\eta_{23}+\eta_{32})^2 + (\eta_{31}+\eta_{13})^2 \tag{38}$$

The constitutive relation cannot simply square the off-diagonal terms individually, because during a pure infinitesimal rotational displacement, the classical displacement components at that point are, for example, $u_1 = -\theta y$ and $u_2 = \theta x$. Then $\eta_{12} = -\theta$ and $\eta_{21} = \theta$ so that

$$\eta_{12} + \eta_{21} \;=\; 0 \qquad\qquad \text{(rigid-body rotation)}$$

So pure rotation stores no strain energy, and yet the expression ${\eta_{12}}^2 + {\eta_{21}}^2$ would be nonzero in such a case. Therefore, (38) is correct, and the general strain energy relation can be written

$$w \;=\; \frac{1}{2}E\sum_i {\eta_{ii}}^2 \;+\; \frac{1}{2}G\sum_{i<j}(\eta_{ij}+\eta_{ji})^2(1-\delta_{ji}). \tag{39}$$

The restriction $i < j$ avoids double counting symmetric pairs since we have already written out the symmetric pairs explicitly. Therefore, the stiffness matrix for isotropic material is

$$K_{ki} \;=\; \begin{cases} G & \text{when } k \neq i \\ E & \text{when } k = i \end{cases} \tag{40}$$

2.4.2 Stress

Taking the derivative $\partial w/\partial \boldsymbol{\xi}$ of (38) yields:

$$\frac{\partial w}{\partial \boldsymbol{\epsilon}} \;=\; \boldsymbol{\sigma} \qquad\qquad \text{and} \qquad\qquad \frac{\partial w}{\partial \boldsymbol{\Gamma}} \;=\; \boldsymbol{\mu}\,, \tag{41}$$

which is Hooke's law and another material constitutive relation involving a moment flux $\boldsymbol{\mu}$. Here, $\boldsymbol{\sigma}$ is the stress at a point in the body. Recall that $\boldsymbol{\Gamma}$ and $\boldsymbol{\epsilon}$ appeared in (33) and have different units.

The following equation calculates both modes of the wrench—rotational (for moments) and translational (for forces):

$$\boldsymbol{\Pi} \;=\; \int_A \frac{\partial w}{\partial \boldsymbol{\xi}}\,\mathrm{d}A \;=\; \begin{bmatrix} \mathbf{M} & \boldsymbol{\omega} \\ 0 & 0 \end{bmatrix}. \tag{42}$$

The reason for this is that strain $\boldsymbol{\xi}$ has two modes according to (33). That is, formula (42) generates a rotational mode, which is torque:

(Moment): $$\mathbf{M} \;=\; \mathbf{\Pi}_{\text{Rot}} \;=\; \int_A \frac{\partial w}{\partial \mathbf{\Gamma}}\,\mathrm{d}A \qquad [\mathrm{N}\cdot\mathrm{m}] \tag{43}$$

and a translational mode, which is force:

(Force): $$\boldsymbol{\omega} \;=\; \mathbf{\Pi}_{\text{Tra}} \;=\; \int_A \frac{\partial w}{\partial \boldsymbol{\epsilon}}\,\mathrm{d}A\,. \qquad [\mathrm{N}] \tag{44}$$

2.4.3 Forces

For the force on a section, we differentiate with respect to the linear mode of (41).

$$\sigma_{ki} \;=\; \frac{\partial w}{\partial \epsilon_{k,i}} \;=\; \frac{\partial w}{\partial \eta_{ki}}\frac{\partial \eta_{ki}}{\partial \epsilon_{i,k}}\,. \tag{45}$$

According to (37),

$$\begin{aligned}\frac{\partial w}{\partial \epsilon_{p,q}} \;&=\; \frac{1}{2}E\sum_i \frac{\partial}{\partial \epsilon_{p,q}}({\eta_{ii}}^2) \;+\; \frac{1}{2}G\sum_{k<i}\frac{\partial}{\partial \epsilon_{p,q}}(\eta_{ki}+\eta_{ik})^2\\ &=\; \frac{1}{2}E\sum_i 2\eta_{ii}\frac{\partial \eta_{ii}}{\partial \epsilon_{p,q}} \;+\; \frac{1}{2}G\sum_{k<i}2(\eta_{ki}+\eta_{ik})\left(\frac{\partial \eta_{ki}}{\partial \epsilon_{p,q}}+\frac{\partial \eta_{ik}}{\partial \epsilon_{p,q}}\right)\end{aligned}$$

When $i \neq k$, the shear term becomes

$$\sum_{k<i}(\eta_{ki}+\eta_{ik})\left(\frac{\partial \eta_{ki}}{\partial \epsilon_{p,q}}+\frac{\partial \eta_{ik}}{\partial \epsilon_{p,q}}\right) \;=\; \sum_{k<i}(\eta_{ki}+\eta_{ik})(\delta_{kp}\delta_{iq}+\delta_{ip}\delta_{kq}) \;=\; (\eta_{pq}+\eta_{qp}) \tag{46}$$

since $\partial\eta_{ki}/\partial\epsilon_{i,k} = 1$. Due to the restriction $(k<i)$, the four terms in the result become only two terms. And once we apply the Kronecker deltas, we can drop the summation sign.

For the normal stress term, we get

$$\sum_i \eta_{ii}\frac{\partial \eta_{ii}}{\partial \epsilon_{i,k}} \;=\; \sum_{i<k}\eta_{ii}\delta_{ik}\,. \tag{47}$$

Putting these two—(47) and (46)—together gives

$$\sigma_{ki} \;=\; \frac{\partial w}{\partial \epsilon_{k,i}} \;=\; E\sum_{k<i}\eta_{ii}\,\delta_{ik} \;+\; G(\eta_{ki}+\eta_{ik})(1-\delta_{ki})\,.$$

So on the diagonal, we have

$$\frac{\partial w}{\partial \epsilon_{i,i}} \;=\; \sigma_{ii} \;=\; E\,\eta_{ii}\,, \tag{48}$$

and when $i \neq k$,

$$\frac{\partial w}{\partial \epsilon_{k,i}} \;=\; \sigma_{ki} \;=\; G(\eta_{ki}+\eta_{ik}) \;=\; G\,\gamma_{ki} \tag{49}$$

where η_{ki} is given by (37). Since

$$\frac{\partial w}{\partial \epsilon_{k,i}} \;=\; \frac{\partial w}{\partial \epsilon_{i,k}}\,,$$

the stress tensor becomes

$$\boldsymbol{\sigma} = \begin{bmatrix} E\,\eta_{11} & G\,(\eta_{12}+\eta_{21}) & G\,(\eta_{13}+\eta_{31}) \\ G\,(\eta_{21}+\eta_{12}) & E\,\eta_{22} & G\,(\eta_{23}+\eta_{32}) \\ G\,(\eta_{31}+\eta_{13}) & G\,(\eta_{32}+\eta_{23}) & E\,\eta_{33} \end{bmatrix} \tag{50}$$

So the force $\boldsymbol{\omega}_i$ acting normal to the section is

$$\omega_i = \int_A \frac{\partial w}{\partial \epsilon_{i,i}} \mathrm{d}A = \int_A E\,\eta_{ii}\,\mathrm{d}A^{(i)} \tag{51}$$

And the force $\boldsymbol{\omega}_k$ acting in direction k on a surface normal to i is

$$\omega_k = \int_A \frac{\partial w}{\partial \epsilon_{k,i}} \mathrm{d}A = \int_A G(\eta_{ki}+\eta_{ik})\,\mathrm{d}A^{(i)}\,, \tag{52}$$

where from (37)

$$\omega_k = \int_A G(\Gamma_{kj,i}\,R_j + \epsilon_{k,i} \;+\; \Gamma_{ij,k}\,R_j + \epsilon_{i,k})\,\mathrm{d}A^{(i)}$$

2.4.4 Moments

Now for the moments, differentiate w in (39) with respect to $\boldsymbol{\Gamma}$ according to (43):

$$\mathbf{M} = \boldsymbol{\Pi}_{\mathrm{Rot}} = \int_A \frac{\partial w}{\partial \boldsymbol{\Gamma}} \mathrm{d}A\,. \tag{53}$$

With basis vectors $\mathbf{e}_p$, $\mathbf{e}_q$, and $\mathbf{e}_r$, the moment flux defined in (41) can be written

$$\boldsymbol{\mu} = \frac{\partial w}{\partial \boldsymbol{\Gamma}} = \frac{\partial w}{\partial \Gamma_{pq,r}} \mathbf{e}_p\,\mathbf{e}_q\,\mathbf{e}_r\,. \tag{54}$$

Let's expand the shear term first:

$$\begin{aligned} \mu_{pq,r} = \frac{\partial w}{\partial \Gamma_{pq,r}} &= G \sum_{k<i} (\eta_{ki}+\eta_{ik}) \left(\frac{\partial \eta_{ki}}{\partial \Gamma_{pq,r}} + \frac{\partial \eta_{ik}}{\partial \Gamma_{pq,r}} \right) \\ &= G \sum_{k<i} (\eta_{ki}+\eta_{ik})(\delta_{kp}\,\delta_{ir}\,R_q + \delta_{ip}\,\delta_{kr}\,R_q) \end{aligned}$$

Once we apply the Kronecker deltas, only one pair of indices contributes, so the summation sign is no longer needed. Recalling from (37) that $\boldsymbol{\eta} = \boldsymbol{\Gamma}\cdot\mathbf{R} + \boldsymbol{\epsilon}$,

$$\begin{aligned} \mu_{pq,r} = \frac{\partial w}{\partial \Gamma_{pq,r}} &= G\,(\eta_{pr}+\eta_{rp})\,R_q\,. \qquad (p \neq r) \\ &= G[(\Gamma_{pj,r}R_j + \epsilon_{p,r}) + (\Gamma_{rj,p}R_j + \epsilon_{r,p})]\,R_q \end{aligned} \tag{55}$$

For the normal part of (39), we have

$$\mu^{(N)}_{pq,r} = \frac{\partial w^{(N)}}{\partial \Gamma_{pq,r}} = E\,\eta_{pp}\,\delta_{pr}\,R_q\,. \qquad (p = r) \tag{56}$$

Therefore, combining (55) and (56) gives

$$\mu_{pq,r} = \begin{cases} E\,\eta_{pp}\,R_q & p = r \\ G\,(\eta_{pr} + \eta_{rp})\,R_q & p \neq r \end{cases} \tag{57}$$

By combining (45) and (57), we can rewrite (41) as one equation, as follows:

$$\nabla w = \boldsymbol{\mu}\,\mathbf{e}_\Gamma + \boldsymbol{\sigma}\,\mathbf{e}_\epsilon = \frac{\partial w}{\partial \boldsymbol{\Gamma}}\mathbf{e}_\Gamma + \frac{\partial w}{\partial \boldsymbol{\epsilon}}\mathbf{e}_\epsilon\,. \tag{58}$$

Here, $\mathbf{e}_\Gamma$ and $\mathbf{e}_\epsilon$ are basis elements of the dual of strain space. The basis element $\mathbf{e}_\Gamma$ has units of 1/m, and the basis element $\mathbf{e}_\epsilon$ is dimensionless.

Notice that in (58) we still have the "conservation of indices" dictated by the quotient rule of tensor analysis. (This rule states that only tensors of the same type may be added together.) But this may not be strictly necessary, as geometric algebra has shown. The quotient rule was abandoned in geometric algebra, where $\mathbf{a}\cdot\mathbf{b}$ and $\mathbf{a}\wedge\mathbf{b}$ are routinely added together even though the second term has two indices, and the first term has none. The notion suggested by (58) is that $\boldsymbol{\mu}$ and $\boldsymbol{\sigma}$ are different grades of a larger object.

It seems likely that the natural setting for mechanics is a 6-dimensional wrench "transmission" form, with a conservation principle of the form:

$$\mathrm{d}\boldsymbol{\Pi} = 0\,.$$

With a single conserved wrench transmission form, beam shear, torsion, bending moments, couple stresses, and forces themselves become manifestations of a single structure.

The pairing of force and moment that has been done in robotics until now has been primarily kinematic, whereas in this formulation, the pairing is constitutive. In robotics, the twist $\mathbf{V} = (\boldsymbol{\Omega}, \mathbf{v})$ and the wrench $\mathbf{W}$ are involved in a power pairing:

$$P = \mathbf{W}\cdot\mathbf{V} = \mathbf{F}\cdot\mathbf{v} + \mathbf{M}\cdot\boldsymbol{\Omega}\,.$$

So the pairing is between motion and load. There is nothing constitutive that is involved.

The pairing that is done in the present formulation is between primary variables $\boldsymbol{\epsilon}$ and $\boldsymbol{\Gamma}$ and the dual objects $\boldsymbol{\sigma}$ and $\boldsymbol{\mu}$. The pairing is not a power pairing but an energy gradient pairing in which the material law has entered through w. The resulting force and moment fields arise as a consequence of a gradient of the strain-energy density *within the material* rather than as externally applied loads.

Robotics pairs loads with motions in $\mathfrak{se}(3)^* \times \mathfrak{se}(3)$, whereas the present theory introduces an analogous constitutive pairing between strain measures and their energetic conjugates in $\mathcal{E}^* \times \mathcal{E}$, where $\mathcal{E}$ is the space of affine distortion generators $\boldsymbol{\eta}$, and $\boldsymbol{\eta}$ is neither a purely translational nor a purely rotational strain gradient. Then $\mathbf{S} = \partial w/\partial\boldsymbol{\xi}$ belongs to the dual space $\mathcal{E}^*$. It appears that $\boldsymbol{\sigma}$ and $\boldsymbol{\mu}$ are merely the projections of $\mathbf{S}$ onto the translational and rotational channels

$$\boldsymbol{\sigma} = \mathbf{S} \qquad \text{and} \qquad \boldsymbol{\mu} = \mathbf{S}\,\mathbf{R}\,, \tag{59}$$

so that $\boldsymbol{\xi} \in \mathcal{E}$ and $\mathbf{S} = \partial w/\partial\boldsymbol{\xi} \in \mathcal{E}^*$.

The conventional moment $\mathbf{r}\wedge\mathrm{d}\boldsymbol{\omega}$ is best suited for computing externally-applied boundary conditions, while

$$\mathrm{d}\mathbf{M} = \boldsymbol{\mu}\cdot\mathrm{d}\mathbf{A} \tag{60}$$

describes internal responses. Then the relation $\mathbf{r}\wedge\mathrm{d}\boldsymbol{\omega} = \mathrm{d}\mathbf{M}$ becomes a compatibility condition between two independently defined objects rather than an identity.

2.4.5 Examples

<u>Example 1. Bending About the x-Axis</u>

Bending Stress

Consider a beam of rectangular cross-section. The task is to obtain expressions for the stress field due to pure bending about the x-axis. If we denote the bending angle as β, then by the same logic used to obtain (25), we compute

$$\mathbf{\Gamma}_{,3} = \mathbf{\Theta}^{-1}\frac{\partial \mathbf{\Theta}}{\partial x} = \begin{bmatrix} 0 & 0 & 0 \\ 0 & 0 & -\beta' \\ 0 & \beta' & 0 \end{bmatrix} = \begin{bmatrix} 0 & 0 & 0 \\ 0 & 0 & -\kappa_x \\ 0 & \kappa_x & 0 \end{bmatrix}, \qquad \mathbf{R} = \begin{bmatrix} x \\ y \\ 0 \end{bmatrix} = \begin{bmatrix} r_1 - \overline{x} \\ r_2 - \overline{y} \\ 0 \end{bmatrix}. \tag{61}$$

Here, κ_x is the beam curvature due to bending, and $\mathbf{R}$ is the position of a point of interest from the centroid. (This centroid can be made to emerge from the solution by minimizing strain energy.)

As seen in (61), the only nonzero component of the rotation gradient is Γ_{23}; therefore, in (37),

$$\mathbf{\Gamma}_{\cdot j,3} R_j = \begin{bmatrix} 0 \\ 0 \\ \kappa_x y \end{bmatrix}. \tag{62}$$

Therefore,

$$\Gamma_{32,3} R_2 = \beta'(z) y = \kappa_x y\,. \tag{63}$$

Then, by substituting (37) into (38), the strain energy due to bending becomes

$$\begin{aligned} w = {} & \frac{1}{2}E(\cancel{\Gamma_{1j,1}}R_j + \cancel{\epsilon_{1,1}})^2 + \frac{1}{2}E(\Gamma_{2j,2}R_j + \cancel{\epsilon_{2,2}})^2 + \frac{1}{2}E(\Gamma_{3j,3}R_j + \epsilon_{3,3})^2 \\ & + \frac{1}{2}G(\cancel{\Gamma_{1j,2}}R_j + \cancel{\epsilon_{1,2}} + \cancel{\Gamma_{2j,1}}R_j + \cancel{\epsilon_{2,1}})^2 + \frac{1}{2}G(\cancel{\Gamma_{1j,3}}R_j + \cancel{\epsilon_{1,3}} + \cancel{\Gamma_{3j,1}}R_j + \epsilon_{3,1})^2 \\ & + \frac{1}{2}G(\Gamma_{2j,3}R_j + \cancel{\epsilon_{2,3}} + \cancel{\Gamma_{3j,2}}R_j + \epsilon_{3,2})^2 \end{aligned}$$

By referring to (61), many of the components of $\mathbf{\Gamma}$ can be seen to be zero and so were crossed out. For example, any components of $\mathbf{\Gamma}$ with a 1 as the first or second index are zero. Many of the strain components are also zero. The above strain energy density then becomes

$$\begin{aligned} w = {} & \frac{1}{2}E(\cancel{\Gamma_{21,2}}R_1 + \cancel{\Gamma_{22,2}}R_2 + \Gamma_{23,2}R_3)^2 + \frac{1}{2}E(\cancel{\Gamma_{31,3}}R_1 + \Gamma_{32,3}R_2 + \cancel{\Gamma_{33,3}}R_3 + \epsilon_{3,3})^2 \\ & + \frac{1}{2}G(\epsilon_{3,1})^2 + \frac{1}{2}G(\cancel{\Gamma_{21,3}}R_1 + \cancel{\Gamma_{22,3}}R_2 + \Gamma_{23,3}R_3 + \epsilon_{3,2})^2 \end{aligned}$$

In fact, since $\Gamma_{kj,r}$ is antisymmetric in the first two indices, things get further simplified:

$$w = \frac{1}{2}E(\Gamma_{32,3}R_2 + \epsilon_{33})^2 + \frac{1}{2}G\,{\epsilon_{31}}^2 + \frac{1}{2}G\,{\epsilon_{32}}^2 \tag{64}$$

So according to (63),

$$\eta_{33} = \Gamma_{32,3}\,y + \epsilon_{33} = \kappa_x y + \epsilon_{33}\,.$$

To compute moments, we take the partial derivative of (64) with respect to $\mathbf{\Gamma}$ as in (43):

$$\mu_{32,3} = \frac{\partial w}{\partial \Gamma_{32,3}} = E\,(\Gamma_{32,3} R_2 + \epsilon_{33}) R_2$$
$$= E\,\kappa_x\, y^2 + E\,\epsilon_{33}\, y$$

We could also write this with basis vectors:

$$\mu_{32,3}\,\mathbf{e}_2\,\mathbf{e}_3\,\mathbf{e}_3 = E\,(\mathbf{e}_3\,\mathbf{e}_3 \Gamma_{32,3} R_2 + \epsilon_{33}\,\mathbf{e}_3\,\mathbf{e}_3) R_2\,\mathbf{e}_2$$
$$= E\,(\kappa_x\, y^2 + \epsilon_{33}\, y)\,\mathbf{e}_3\,\mathbf{e}_3\,\mathbf{e}_2$$

Then, the moment in (42) becomes

$$\mathbf{M}_x = \int_A \boldsymbol{\mu}\cdot \mathrm{d}\mathbf{A} = E\int_A \mu_{32,3}\,\mathbf{e}_2\,\mathbf{e}_3\,\mathbf{e}_3\cdot\mathbf{e}_3\,\mathrm{d}A$$
$$= E\,\mathbf{e}_2\,\mathbf{e}_3 \int_A (\kappa_x\, y^2 + \epsilon_{3,3}\, y)\,\mathrm{d}A$$
$$= E\,\mathbf{e}_2\,\mathbf{e}_3 \int_A \kappa_x\, y^2\,\mathrm{d}A + E\,\epsilon_{3,3}\,\mathbf{e}_3\,\mathbf{e}_2 \int_A y\,\mathrm{d}A \tag{65}$$

The second integral vanishes if R_2 is defined from the centroid. The term survives if the origin is not centered or if there is eccentric axial loading. Consequently, the present formulation may contain some coupling physics that classical beam theory removes. A variational energy minimizing procedure selects the centroid in this case.

The moment is then

$$\mathbf{M}_x = E\int_A \kappa_x\, y^2 (\mathbf{e}_2 \wedge \mathbf{e}_3)\,\mathrm{d}A$$
$$\mathbf{M}_x = E\kappa_x \int_{-h/2}^{h/2}\int_{-b/2}^{b/2} y^2\,\mathbf{e}_2\wedge\mathbf{e}_3\,\mathrm{d}x\,\mathrm{d}y$$
$$\mathbf{M}_x = E\kappa_x \frac{bh^3}{12}\,\mathbf{e}_2\wedge\mathbf{e}_3 \tag{66}$$

The moment is a bivector in the $\mathbf{e}_2\wedge\mathbf{e}_3$ plane. Its magnitude is

$$M_x = E\,\kappa_x\, I_x\,, \tag{67}$$

where I_x is the area moment of inertia about the x-axis. From Hooke's law (48), we have $\sigma = E\,\epsilon$ so that

$$\sigma = \frac{M_x\,\epsilon_{33}}{\kappa_x\, I_x}\,. \tag{68}$$

The following is a one-line proof that $\epsilon_{33} = y\,\kappa_x$ in a beam with ρ as the radius of curvature:

$$\epsilon_{33} = \frac{\text{change in length}}{\text{original length}} = \frac{\mathrm{d}l(y) - \mathrm{d}z(y_c)}{\mathrm{d}z(y_c)} = \frac{(\rho+y)\mathrm{d}\theta - \mathrm{d}z}{\rho\,\mathrm{d}\theta} = \frac{(\rho+y)}{\rho} - 1 = \frac{y}{\rho} = y\,\kappa_x\,,$$

from which (68) becomes the classical formula:

$$\sigma_{33} = \frac{M_x\, y}{I_x}\,. \tag{69}$$

Shear in Bending

The conventional derivation of the shear stress in beams is typically a tedious process involving diagrams, intuitive arguments about forces needing somewhere to go, and nested integrals. We are expected to notice that the axial force in the upper part of the beam changes from one section to the next, and therefore there must be a horizontal shear stress. A notion that can remove some of this tedium, or at least make it worthwhile, is the realization that there is a relatively profound guiding principle involved. The most mysterious step in the derivation can be boiled down to an application of Stokes' theorem which states that for any sufficiently smooth domain Ω,

$$\int_{\partial\Omega} \omega \;=\; \int_{\Omega} \mathrm{d}\omega\,. \tag{70}$$

To see it in action, consider the axial force 2-form (in the z direction):

$$\omega_3 \;=\; \sigma_{31}\,\mathrm{d}y\wedge\mathrm{d}z \;+\; \sigma_{32}\,\mathrm{d}z\wedge\mathrm{d}x \;+\; \sigma_{33}\,\mathrm{d}x\wedge\mathrm{d}y \tag{71}$$

Note that σ_{31}, for example, is just a scalar coefficient, not a 2-form. It is the force that is the 2-form. Having a force, which is a vector, with components that are 2-forms is just as peculiar, but in the opposite sense, as the traction vector, which has units of stress, and yet is a 1-form (it is created by dotting the stress with a dimensionless normal vector). So we could say that force is a vector-valued 2-form

$$\boldsymbol{\omega} = \mathbb{R}^3 \otimes \wedge^2\,,$$

while the traction vector is a force-valued density on a surface. Classical mechanics often starts with point particles, while continuum mechanics suggests that stress over an area is a more fundamental notion. Since $\dim(\mathbb{R}^3) = 3$ and $\dim(\wedge^2) = 3$, the total number of elements involved in this description is $3\times 3 = 9$, which is the same as that of the stress tensor. The 2-form description of force components reveals structure that is harder to see with vector notation alone. If we expand the discussion to the wrench, we could write

$$\boldsymbol{\Pi} = \mathbb{R}^6 \otimes \wedge^2\,,$$

which could be referred to as a wrench-valued 2-form—a six-component mechanical object whose entries are transmission forms.

Returning to the task at hand, since no net z-directed force is being created, destroyed, or accumulated within the volume element $\mathrm{d}x\wedge\mathrm{d}y\wedge\mathrm{d}z$, the differential of ω_3 in (71) is the closed form

$$\mathrm{d}\omega_3 \;=\; 0\,. \tag{72}$$

This is a conservation statement, and it also happens to lead to the equilibrium equation. One of the terms in (71) is the axial bending stress from (69). And shear stress exists because the force 2-form ω_3 must remain closed. Expanding (72) gives

$$\begin{aligned}\mathrm{d}\omega_3 \;&=\; \mathrm{d}(\sigma_{31}\,\mathrm{d}y\wedge\mathrm{d}z) \;+\; \mathrm{d}(\sigma_{32}\,\mathrm{d}z\wedge\mathrm{d}x) \;+\; \mathrm{d}(\sigma_{33}\,\mathrm{d}x\wedge\mathrm{d}y) \;=\; 0\\ &=\; \partial_x(\sigma_{31})\mathrm{d}x\wedge\mathrm{d}y\wedge\mathrm{d}z \;+\; \partial_y(\sigma_{32})\,\mathrm{d}y\wedge\mathrm{d}z\wedge\mathrm{d}x \;+\; \partial_z(\sigma_{33})\,\mathrm{d}z\wedge\mathrm{d}x\wedge\mathrm{d}y,\end{aligned}$$

since $\mathrm{d}x\wedge\mathrm{d}x = \mathrm{d}y\wedge\mathrm{d}y = \mathrm{d}z\wedge\mathrm{d}z = 0$. The resulting closure condition

$$\mathrm{d}\omega_3 \;=\; (\partial_x\sigma_{31} + \partial_y\sigma_{32} + \partial_z\sigma_{33})\,\mathrm{d}x\wedge\mathrm{d}y\wedge\mathrm{d}z \;=\; 0 \tag{73}$$

requires that

$$\partial_x \sigma_{31} + \partial_y \sigma_{32} + \partial_z \sigma_{33} \;=\; 0 \tag{74}$$

(This is the equilibrium equation.) For bending entirely in the y-z plane, $\partial_x(\;) = 0$ because in the x direction, all sections through the entire beam look identical. Using this simplification, the closure condition can be integrated to obtain

$$\int \frac{\partial \sigma_{32}}{\partial y}\,\mathrm{d}A \;=\; -\int \frac{\partial \sigma_{33}}{\partial z}\,\mathrm{d}A\,.$$

Using Stokes' theorem to rewrite the integral on the left as a line integral around the area, and using the stress in (69) on the right side, gives

$$\oint_{\partial A} \sigma_{32}\,\mathrm{d}s \;=\; -\int_A \frac{\partial}{\partial z}\left(\frac{M_x(z)\,y}{I_x}\right)\mathrm{d}A$$

$$\underbrace{\int_{s_1} \sigma_{32}\,\mathrm{d}s}_{\substack{\text{Along side.}\\ \text{Free surface}}} + \underbrace{\int_{s_2} \sigma_{32}\,\mathrm{d}s}_{\substack{\text{Along } b.\\ \text{Free surface}}} + \underbrace{\int_{s_3} \sigma_{32}\,\mathrm{d}s}_{\substack{\text{Along side.}\\ \text{Free surface}}} + \underbrace{\int_{s_4} \sigma_{32}\,\mathrm{d}s}_{\substack{\text{Along } b.\\ \text{(Of interest)}}} \;=\; -\frac{1}{I_x}\frac{\mathrm{d}M_x(z)}{\mathrm{d}z}\int_A y\,\mathrm{d}A \tag{75}$$

One of the assumptions usually cited in deriving beam shear stress is that it remains constant along the beam width b. However, as shown in the left side of the above relation, this assumption is stricter than needed. The desired simplification of the contour integral around the section between the y-value of interest and the free surface only requires that the stresses along legs 1 and 3 vary in the same way, not that they not vary at all. This then allows them to be cancelled out. The sectional area to be integrated can actually be on either side of the y-value of interest because the two sides will be equal and opposite. The smaller of the two is simpler and therefore usually recommended.

The integral on the far right of (75)—the first moment of area—is usually denoted as Q. We know from shear and bending moment diagrams that $\mathrm{d}M/\mathrm{d}z = V$, where V is the shear force. With these substitutions and the fact that the shear stress must be zero at the free surface, (75) reduces to

$$\int_{s_1} \sigma_{32}\,\mathrm{d}s \;+\; (0)b \;-\; \int_{s_1} \sigma_{32}\,\mathrm{d}s \;-\; \sigma_{32}\,b \;=\; -\frac{VQ}{I_x}\,,$$

so the bending shear closure stress is

$$\sigma_{32} \;=\; \frac{VQ}{I_x\,b}\,, \tag{76}$$

which is the classical formula for the shear stress in a beam.

The classical beam shear formula arose from solving the closure equation on a subdomain of the cross-section. So while the shear stress appears entirely unrelated to the axial bending stress, shear is the flux component required to make ω_3 closed. This effect is depicted below in the strain gradient matrix $\boldsymbol{\eta}$:

$$\boldsymbol{\eta} = \begin{bmatrix} 0 & 0 & 0 \\ 0 & 0 & 0 \\ 0 & 0 & \eta_{33} \end{bmatrix} \;\rightarrow\; \begin{bmatrix} 0 & 0 & 0 \\ 0 & 0 & 0 \\ 0 & \eta_{32} & \eta_{33} \end{bmatrix} = \begin{bmatrix} 0 & 0 & 0 \\ 0 & 0 & 0 \\ 0 & \sigma_{32}/G & \Gamma_{32,3}y \end{bmatrix} \tag{77}$$

Example 2. Circular Shaft in Pure Torsion About z-Axis

Now suppose a circular shaft is in pure torsion about the z-axis (or in the x-y plane). As shown in (25), the rotational strain gradient $\mathbf{\Gamma}_{,3}$ about the z-axis is given by

$$\mathbf{R} = \begin{bmatrix} x \\ y \\ 0 \end{bmatrix}, \qquad \mathbf{\Gamma}_{,3} = \begin{bmatrix} \Gamma_{11,3} & \Gamma_{12,3} & \Gamma_{13,3} \\ \Gamma_{21,3} & \Gamma_{22,3} & \Gamma_{23,3} \\ \Gamma_{31,3} & \Gamma_{32,3} & \Gamma_{33,3} \end{bmatrix} = \begin{bmatrix} 0 & -\phi' & 0 \\ \phi' & 0 & 0 \\ 0 & 0 & 0 \end{bmatrix}. \tag{78}$$

Here, ϕ is the angle of twist of the shaft. For torsion, the rotation gradient

$$\phi'(z) = \kappa_z \tag{79}$$

goes by various names, including the angle gradient $\nabla\phi$ and the curvature $\boldsymbol{\kappa}_z$ in the z direction due to torsion.

To compute the strain gradient in (37), take the product of $\mathbf{\Gamma}_{,3}$ and $\mathbf{R}$ given in (78) and obtain

$$\boldsymbol{\eta}_{,3} = \mathbf{\Gamma}_{\cdot p,3} R_p = \begin{bmatrix} \Gamma_{12,3}\, y \\ \Gamma_{21,3}\, x \\ 0 \end{bmatrix} = \phi' \begin{bmatrix} -y \\ x \\ 0 \end{bmatrix}. \tag{80}$$

So the full matrix $\boldsymbol{\eta}$ is

$$\boldsymbol{\eta} = \begin{bmatrix} 0 & 0 & -\phi' y \\ 0 & 0 & \phi' x \\ 0 & 0 & 0 \end{bmatrix},$$

and the two important components are

$$\eta_{13} = \Gamma_{12,3}\, y = -\phi' y\,, \tag{81}$$

$$\eta_{23} = \Gamma_{21,3}\, x = \phi' x\,. \tag{82}$$

The axial strains are zero, and $\epsilon_{i,k} = 0$ for all i and k, so (38) reduces to

$$\begin{aligned} w &= \frac{1}{2} G[(\eta_{23} + \cancel{\eta_{32}})^2 + (\cancel{\eta_{31}} + \eta_{13})^2] = \frac{1}{2} G({\eta_{23}}^2 + {\eta_{13}}^2) \\ &= \frac{1}{2} G[(\Gamma_{21,3}\, x)^2 + (\Gamma_{12,3}\, y)^2] \end{aligned} \tag{83}$$

Since the shaft is circular, there is no Saint-Venant warping, so $\epsilon_{3,1} = \epsilon_{3,2} = 0$. Therefore, the translational strains were crossed out.

Moments

The integrand of the moment given by (42)

$$\mathbf{M} = \int_A \frac{\partial w}{\partial \mathbf{\Gamma}} \mathrm{d}A \tag{84}$$

can be written

$$\boldsymbol{\mu} = \frac{\partial w}{\partial \mathbf{\Gamma}} = \mu_{pq,r}\, \mathbf{e}_p\, \mathbf{e}_q\, \mathbf{e}_r\,.$$

From (57), this becomes

$$\boldsymbol{\mu} = \frac{\partial w}{\partial \boldsymbol{\Gamma}} = G(\eta_{pr} + \eta_{rp}) R_q \, \mathbf{e}_p \, \mathbf{e}_q \, \mathbf{e}_r$$

or

$$\begin{aligned} \mu_{pq,r} &= G(\eta_{pr} + \eta_{rp}) R_q \\ &= G(\Gamma_{pj,r} R_j + \cancel{\epsilon_{p,r}} + \Gamma_{rj,p} R_j + \cancel{\epsilon_{r,p}}) R_q \end{aligned} \tag{85}$$

Since there is no Saint-Venant warping, the translational strains were again crossed out.

Then for the axial direction, let the index $r = 3$:

$$\boldsymbol{\mu}_{,3} = \frac{\partial w}{\partial \boldsymbol{\Gamma}_{,3}} = \mu_{pq,3} \, \mathbf{e}_p \, \mathbf{e}_q \, \mathbf{e}_3 \, .$$

This expands as

$$\boldsymbol{\mu}_{,3} = \mu_{11,3} \, \mathbf{e}_1 \, \mathbf{e}_1 \, \mathbf{e}_3 + \mu_{12,3} \, \mathbf{e}_1 \, \mathbf{e}_2 \, \mathbf{e}_3 + \mu_{21,3} \, \mathbf{e}_2 \, \mathbf{e}_1 \, \mathbf{e}_3 + \mu_{22,3} \, \mathbf{e}_2 \, \mathbf{e}_2 \, \mathbf{e}_3 \, . \tag{86}$$

Each component of $\boldsymbol{\mu}_{,3}$ will be calculated individually. First, let $p = 1$ and $q = 1$ in (85):

$$\begin{aligned} \mu_{11,3} &= G(\Gamma_{1j,3} R_j + \cancel{\Gamma_{3j,1} R_j}) R_1 \\ &= G(\cancel{\Gamma_{11,3}} R_1 + \Gamma_{12,3} R_2 + \Gamma_{13,3} \cancel{R_3}) R_1 \\ &= G(\Gamma_{12,3} R_2) R_1 \\ &= G(-\phi' y) x \end{aligned}$$

Several Γs could be crossed out by referring to (78).

Likewise, for $q = 2$,

$$\begin{aligned} \mu_{12,3} &= G(\Gamma_{1j,3} R_j + \cancel{\Gamma_{3j,1} R_j}) R_2 \\ &= G(\cancel{\Gamma_{11,3}} R_1 + \Gamma_{12,3} R_2 + \Gamma_{13,3} \cancel{R_3}) R_2 \\ &= G(\Gamma_{12,3} R_2) R_2 \\ &= G(-\phi' y) y \end{aligned}$$

For $p = 2$ and $q = 1$,

$$\begin{aligned} \mu_{21,3} &= G(\Gamma_{2j,3} R_j + \cancel{\Gamma_{3j,2} R_j}) R_1 \\ &= G(\Gamma_{21,3} R_1 + \cancel{\Gamma_{22,3}} R_2 + \Gamma_{23,3} \cancel{R_3}) R_1 \\ &= G(\phi' x) x \end{aligned}$$

and finally,

$$\begin{aligned} \mu_{22,3} &= G(\Gamma_{2j,3} R_j + \cancel{\Gamma_{3j,2} R_j}) R_2 \\ &= G(\Gamma_{21,3} R_1 + \cancel{\Gamma_{22,3}} R_2 + \Gamma_{23,3} \cancel{R_3}) R_2 \\ &= G(\Gamma_{21,3} R_1) R_2 \\ &= G(\phi' x) y \end{aligned}$$

Substituting these four values into (86) gives

$$\begin{aligned}
\boldsymbol{\mu} &= \mu_{11,3}\,\mathbf{e}_1\,\mathbf{e}_1\,\mathbf{e}_3 \;+\; \mu_{12,3}\,\mathbf{e}_1\,\mathbf{e}_2\,\mathbf{e}_3 \;+\; \mu_{21,3}\,\mathbf{e}_2\,\mathbf{e}_1\,\mathbf{e}_3 \;+\; \mu_{22,3}\,\mathbf{e}_2\,\mathbf{e}_2\,\mathbf{e}_3 \\
&= -\,G\,\phi' xy\,\mathbf{e}_1\,\mathbf{e}_1\,\mathbf{e}_3 - G\phi' y^2\,\mathbf{e}_1\,\mathbf{e}_2\,\mathbf{e}_3 \;+\; G\phi' x^2\,\mathbf{e}_2\,\mathbf{e}_1\,\mathbf{e}_3 \;+\; G\phi' xy\,\mathbf{e}_2\,\mathbf{e}_2\,\mathbf{e}_3 \\
&= -\,G\,\phi' xy\,\mathbf{e}_3 - G\phi' y^2\,\mathbf{e}_1\,\mathbf{e}_2\,\mathbf{e}_3 \;-\; G\phi' x^2\,\mathbf{e}_1\,\mathbf{e}_2\,\mathbf{e}_3 \;+\; G\phi' xy\,\mathbf{e}_3 \qquad (87)
\end{aligned}$$

$$\boldsymbol{\mu} = -\,G\phi' R^2\,\mathbf{e}_1\,\mathbf{e}_2\,\mathbf{e}_3 \qquad (88)$$

Then, according to (59), the stress at any point in the cross-sectional area is

$$\boldsymbol{\sigma} = \boldsymbol{\mu}/\mathbf{R} = -\,G\phi' R\,\mathbf{e}_1\,\mathbf{e}_3 \quad \text{or} \quad -\,G\phi' R\,\mathbf{e}_2\,\mathbf{e}_3\,. \qquad (89)$$

The moment in the area due to torsion is found by (53) or (60)

$$\mathbf{M} = \int_A \boldsymbol{\mu}\cdot \mathrm{d}\mathbf{A}\,. \qquad (90)$$

If we consider area to be represented vectorially by its normal vector $\mathbf{e}_3$, then

$$\begin{aligned}
\mathbf{M} &= -\,G\phi' \int_A R^2\,\mathbf{e}_1\,\mathbf{e}_2\,\mathbf{e}_3\cdot\mathbf{e}_3\,\mathrm{d}A \\
&= -\,G\phi' \int_A R^2\,\mathbf{e}_1\,\mathbf{e}_2\,\mathrm{d}A\,, \qquad (91)
\end{aligned}$$

and the moment occupies the $\mathbf{e}_1\,\mathbf{e}_2$ plane. Conversely, if the area is represented by the bivector $\mathbf{e}_1\,\mathbf{e}_2$, then the moment's direction is represented by the $\mathbf{e}_3$ basis vector. The area is the cross-section of a circular shaft; therefore,

$$\mathbf{M} = G\,\phi'\mathbf{e}_1\,\mathbf{e}_2 \int_R\int_\theta R^2 R\,\mathrm{d}\theta\mathrm{d}R \qquad (92)$$

Integrate the stress above over the cross-sectional area. Then the moment about the z-axis is

$$\mathbf{M} = G\phi'\,\frac{\pi R^4}{2}(\mathbf{e}_1\wedge\mathbf{e}_2)$$

Its magnitude is the classical formula for a circular shaft in torsion:

$$\left|\mathbf{M}\right| = G\,\phi'\,\frac{\pi R^4}{2} = G\,\phi'\,I_P\,. \qquad (93)$$

Stresses

To find the stresses, use (50) and (48), with (37), as follows:

$$\begin{aligned}
\sigma_{ii} &= \frac{\partial w}{\partial \epsilon_{i,i}} = E\,\eta_{ii} & \sigma_{ki} &= \frac{\partial w}{\partial \epsilon_{k,i}} = G(\eta_{ki}+\eta_{ik}) \equiv G\,\gamma_{ki} \\
&= E(\Gamma_{ij,i}\,R_j \;+\; \epsilon_{i,i}) & &= G\,(\Gamma_{kj,i}\,R_j + \epsilon_{k,i} \;+\; \Gamma_{ij,k}\,R_j + \epsilon_{i,k})
\end{aligned}$$

Therefore, from (81) and (82),

$$\sigma_{13} = G\,\gamma_{13} = -\,G\,\phi' y \qquad (94)$$

$$\sigma_{23} = G\,\gamma_{23} = G\,\phi' x \qquad (95)$$

This is Hooke's law, which says that shear stress is $\tau = GR\phi'$. Now write

$$\tau = \sqrt{{\sigma_{13}}^2 + {\sigma_{23}}^2} = G\phi'\sqrt{x^2+y^2}\,,$$

and substitute (93) to get the classical engineering formula for shear stress in a circular shaft:

$$\tau \;=\; \frac{M_T\, R}{I_P}\,. \tag{96}$$

<u>Example 3. Rubber Block Under Combined Loads</u>

Consider a rubber block with the following geometry, material properties, and combined loads:

Material and geometry:

Block: $W = 0.02\,\mathrm{m},\ H = 0.05\,\mathrm{m},\ L = 0.2\,\mathrm{m}$ (x, y, and z directions)
Material: Rubber. $E = 30$ MPa; $G = 10$ MPa
Axial: F = 5 N, compression (in the z-direction)
Bending: $\mathbf{F}(L) \;=\; 30\ \mathrm{N}\,\mathbf{e}_y$ (about the x-axis)
Torque: $-5\ \mathrm{N}\cdot\mathrm{m}$ (about the z-axis)
Domain of material: $-\dfrac{W}{2} \le x \le \dfrac{W}{2}\,,\qquad -\dfrac{H}{2} \le y \le \dfrac{H}{2}$

Define the special vector $\mathbf{R}$ to be used in (36) as:

$$\mathbf{R} \;=\; \begin{bmatrix} x \\ y \\ 0 \end{bmatrix} \;=\; \begin{bmatrix} r_1 - \overline{x} \\ r_2 - \overline{y} \\ 0 \end{bmatrix}.$$

Stresses

To find the stresses, use (50) and (48), with (37), as follows:

$$\begin{aligned} \sigma_{ii} \;&=\; \frac{\partial w}{\partial \epsilon_{i,i}} \;=\; E\,\eta_{ii} & \qquad \sigma_{ki} \;&=\; \frac{\partial w}{\partial \epsilon_{k,i}} \;=\; G(\eta_{ki} + \eta_{ik}) \;=\; G\,\gamma_{ki} \\ &= E(\Gamma_{ij,i}\,R_j \;+\; \epsilon_{i,i}) & &=\; G\,(\Gamma_{kj,i}\,R_j + \epsilon_{k,i} \;+\; \Gamma_{ij,k}\,R_j + \epsilon_{i,k}) \end{aligned} \tag{97}$$

Axial Strain

Axial strain is straightforward:

$$\epsilon(z)\,\mathbf{e}_z\,.$$

Its gradient is

$$\boldsymbol{\epsilon}_{,3}(z) = \partial_z \boldsymbol{\epsilon}(z)\,.$$

So by (48),

$$\epsilon_{33} = \frac{F_z}{EA}\,. \tag{98}$$

Bending

We saw in (77) that for bending about the x-axis, the strain gradient matrix was equal to

$$\boldsymbol{\eta}^{(x)} \;=\; \begin{bmatrix} 0 & 0 & 0 \\ 0 & 0 & 0 \\ 0 & \eta_{32} & \eta_{33}{}^{(x)} \end{bmatrix},$$

with $\eta_{33}{}^{(x)} = \Gamma_{32,3}{}^{(x)} R_2 = \kappa_x\, y$ according to (63), and the off-diagonal determined by the closure condition (74). Similarly, for bending about the y-axis, we would have

$$\boldsymbol{\eta}^{(y)} = \begin{bmatrix} 0 & 0 & 0 \\ 0 & 0 & 0 \\ \eta_{31} & 0 & \eta_{33}{}^{(y)} \end{bmatrix}$$

with the off-diagonal determined by the closure condition. Therefore,

$$\eta_{33}{}^{(x)} = \Gamma_{32,3}{}^{(x)} R_2 = \kappa_x\, y \qquad\qquad \eta_{33}{}^{(y)} = \Gamma_{31,3}{}^{(y)} R_1 = -\kappa_y\, x \tag{99}$$

The total is the component-wise sum of these two strain gradients:

$$\begin{aligned} \eta_{33} &= \Gamma_{3j,3} R_j + \epsilon_{3,3} \\ &= \Gamma_{31,3} R_1 + \Gamma_{32,3} R_2 + \epsilon_{3,3} \\ &= -\kappa_y\, x \;+\; \kappa_x\, y \;+\; \epsilon_{3,3} \end{aligned}$$

and

$$\boldsymbol{\eta} = \begin{bmatrix} 0 & 0 & 0 \\ 0 & 0 & 0 \\ \eta_{31} & \eta_{32} & \eta_{33} \end{bmatrix} = \begin{bmatrix} 0 & 0 & 0 \\ 0 & 0 & 0 \\ \eta_{31} & \eta_{32} & (\kappa_x\, y - \kappa_y x + \epsilon_{3,3}) \end{bmatrix}.$$

So the normal stress is

$$\sigma_{33} \;=\; E\,\eta_{33} \;=\; E(\kappa_x\, y - \kappa_y x + \epsilon_{3,3}) \tag{100}$$

This stress is shown in Figure 1.

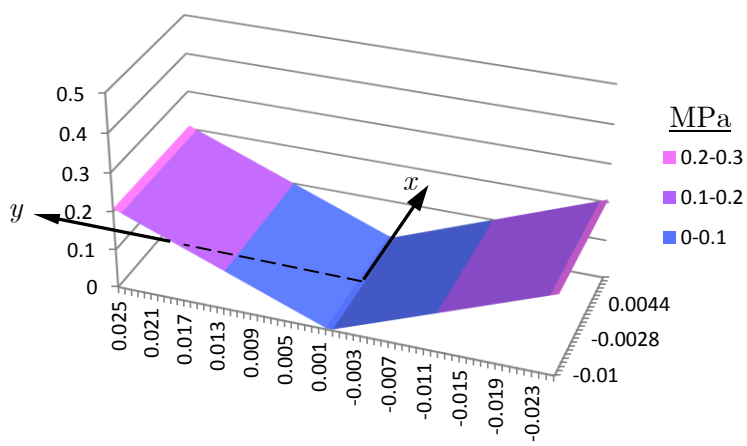

Figure 1. Bending stress in the rubber block of Example 3 (bending about the x-axis only) at the section at the mid-span ($z = 0.1\,\mathrm{m}$).

Closure-Generated Bending Shear

The z-force 2-form is, as in the (71),

$$\omega_3 \;=\; \sigma_{31}\,\mathrm{d}y\wedge\mathrm{d}z \;+\; \sigma_{32}\,\mathrm{d}z\wedge\mathrm{d}x \;+\; \sigma_{33}\,\mathrm{d}x\wedge\mathrm{d}y\,. \tag{101}$$

This time, the closedness condition $\mathrm{d}\omega_3 = 0$ governs all z-directed transmission, not only bending, so (74) is written:

$$\partial_x(\underset{T}{\sigma_{31}} + \underset{B^{(y)}}{\sigma_{31}}) + \partial_y(\underset{T}{\sigma_{32}} + \underset{B^{(x)}}{\sigma_{32}}) + \partial_z\sigma_{33} \;=\; 0\,. \tag{102}$$

In combined loading, the closure condition on ω_3 generates shear $\underset{B^{(x)}}{\sigma_{32}}$ due to bending about the x-axis, and constrains the torsional shear $\underset{T}{\sigma_{32}}$.

First, perform the differentiation of (100) required by (102):

$$\partial_z\sigma_{33} \;=\; E(\epsilon'_{33} \;+\; \kappa'_x\,y \;-\; \kappa'_y x)$$

Then, the closure-generated shear stresses must satisfy

$$\partial_x(\underset{T}{\sigma_{31}} + \underset{B^{(y)}}{\sigma_{31}}) + \partial_y(\underset{T}{\sigma_{32}} + \underset{B^{(x)}}{\sigma_{32}}) \;=\; -\,E(\epsilon'_{33} \;+\; \kappa'_x\,y \;-\; \kappa'_y x) \tag{103}$$

This equation and the boundary conditions determine σ_{31} and σ_{32}.

Up to this point, the formulation has been kept general enough to allow for bending about both the x and y axes as well as torsion about z and axial compression. If we focus briefly on bending, (103) becomes

$$\partial_x{\sigma_{31}}^{(y)} + \partial_y{\sigma_{32}}^{(x)} \;=\; -\,E(\kappa'_x\,y \;-\; \kappa'_y x)\,,$$

which can be partitioned into two separate shear problems.

$$\partial_y{\sigma_{32}}^{(x)} \;=\; -\,E\,\kappa'_x\,y \qquad\qquad \partial_x{\sigma_{31}}^{(y)} \;=\; E\,\kappa'_y x$$

Then integrate

$${\sigma_{32}}^{(x)} \;=\; -\frac{1}{2}E\,\kappa'_x\,y^2 + c_1(x,z) \qquad\qquad {\sigma_{31}}^{(y)} \;=\; \frac{1}{2}E\,\kappa'_y x^2 + c_2(y,z)$$

Imposing a zero shear traction on surfaces of the rectangular section

$${\sigma_{32}}^{(x)}\Big|_{\pm H/2} = 0 \qquad\qquad {\sigma_{31}}^{(y)}\Big|_{\pm W/S} = 0$$

gives

$$\sigma_{32} = \frac{1}{2}E\,\kappa'_x\left(\frac{H^2}{4} - y^2\right) \qquad\qquad \sigma_{31} = \frac{1}{2}E\,\kappa'_y\left(x^2 - \frac{W^2}{4}\right) \tag{104}$$

The corresponding shear gradient components are:

$$\gamma_{23} \;=\; \cancel{\eta_{23}} + \eta_{32} \;=\; \frac{\sigma_{32}}{G} \qquad\qquad \gamma_{13} \;=\; \cancel{\eta_{13}} + \eta_{31} \;=\; \frac{\sigma_{31}}{G} \tag{105}$$

The shear stress in (104) due to bending about the x axis is shown in Figure 2.

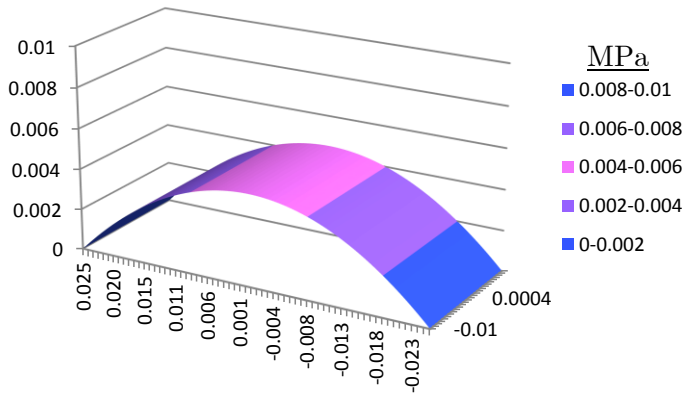

Figure 2. Shear stress in the rubber block of Example 3 at the section at the mid-span ($z = 0.1\,\mathrm{m}$) due to bending about the x-axis.

Torsion

When the cross section is not circular, the torsional stiffness depends on direction from the centroid. This non-uniform stiffness causes warping in the axial direction, as Saint-Venant discovered (Saint-Venant 1856). However, this too is a result of the closure criterion $\mathrm{d}\omega_3 = 0$ in (72). This will be shown shortly.

The torsion can be put in the usual form by substituting (94) and (95) into (87) and the result into (90). This gives

$$\mathbf{M} \;=\; \int_A (\sigma_{13}\, y \;-\; \sigma_{23}\, x)\, \mathbf{e}_1\, \mathbf{e}_2\, \mathrm{d}\mathbf{A} \tag{106}$$

Define the Prandtl stress function φ as

$$\sigma_{13} = \varphi_{,2} \qquad \text{and} \qquad \sigma_{23} = -\varphi_{,1} \tag{107}$$

so that the equilibrium or closure condition (74), written while invoking symmetry as

$$\partial_x \sigma_{13} + \partial_y \sigma_{23} \;=\; 0\,,$$

is satisfied identically (analogous to the streamfunction in fluid mechanics). This allows us to write the magnitude of the torque in (106) as

$$M \;=\; \int_A (\varphi_{,2}\, y \;+\; \varphi_{,1}\, x)\, \mathrm{d}A \tag{108}$$

This form motivates one to write the following identity:

$$\nabla \cdot \begin{bmatrix} x\varphi \\ y\varphi \end{bmatrix} \;=\; x\varphi_{,1} + y\varphi_{,2} \;+\; 2\varphi$$

because the first two terms on the right side can be substituted into (108) to give

$$M \;=\; \int_A \nabla \cdot \begin{bmatrix} x\varphi \\ y\varphi \end{bmatrix} \mathrm{d}A \;-\; \int_A 2\varphi\, \mathrm{d}A\,.$$

Applying Stokes' theorem to the integral on the left allows us to write it as an integral over the boundary of the section with $\mathbf{n}$ as the unit vector normal to *the boundary of* the section:

$$M \;=\; \int_{\partial A} \varphi(xn_1 + yn_2)\,\mathrm{d}s \;-\; \int_A 2\varphi\,\mathrm{d}A \tag{109}$$

The first integral on the right side will be zero for several different boundary conditions:

1. φ is zero on the boundary ∂A, or perimeter, of the cross-section, (Dirichlet case)
2. φ has symmetry cancellation on boundary ∂A
3. φ is chosen so that its projection at the boundary onto $(\mathbf{r}\cdot\mathbf{n})$ is orthogonal [each individual mode of the Galerkin/Fourier series with cosine base vanishes]
4. The Galerkin system generates coefficients that cancel in the weighted sum, even if individual modes do not vanish

For the present example of a rubber block with a rectangular cross-section, the boundary term in (109) will be annihilated (below) not because $\varphi = 0$ on the boundary but because of #3 and #4 above—the cosine basis to be used in the Galerkin/Fourier series for φ will restrict φ to a subspace in which the boundary integral has no independent degrees of freedom, and the Galerkin system will enforce this constraint through its coefficients.

With the boundary integral in (109) eliminated by one or more of the 4 conditions listed above, it becomes

$$M \;=\; 2\int_A \varphi\,\mathrm{d}A\,. \tag{110}$$

But this equation is not enough to completely determine the coefficients of a series solution for φ for the rectangular cross-section. As implied by the four conditions listed above infinitely many φ's satisfy the same torque integral. To solve for φ, we need another governing equation [(118) below]. This comes from the compatibility equation.

Compatibility

Compatibility asks whether there exists a configuration field $\mathbf{X}$ producing the strain in question. The compatibility equations are the conditions that guarantee this. Compatibility says that the strain field is locally exact, but it is usually expressed by showing that an associated differential form is closed. The Maurer–Cartan equation

$$\mathrm{d}\boldsymbol{\xi} \;+\; \boldsymbol{\xi}\wedge\boldsymbol{\xi} \;=\; 0 \tag{111}$$

is more fundamental than the classical compatibility equations. For ordinary (Abelian) differential forms ω, integrability is expressed by the closure condition $\mathrm{d}\omega = 0$ as we saw in Example 1. But for Lie-algebra-valued forms associated with a noncommutative group, noncommutativity introduces the additional term $\boldsymbol{\xi}\wedge\boldsymbol{\xi}$, yielding the Maurer–Cartan integrability condition (111) (Helgason 1978). So the Maurer–Cartan equation may be viewed as the noncommutative generalization of the closure condition $\mathrm{d}\omega = 0$. In the Abelian limit, $\boldsymbol{\xi}\wedge\boldsymbol{\xi} = 0$, and the Maurer–Cartan equation reduces exactly to $\mathrm{d}\boldsymbol{\xi} = 0$.

The quadratic term in (111) appears because SE(3) is noncommutative. And it is the rotational part $\boldsymbol{\Gamma}$ of the Lie algebra that causes the noncommutativity (rotations do not commute).

Suppose a strain $\boldsymbol{\xi}$ satisfies the Maurer–Cartan form $\boldsymbol{\xi} = \mathbf{X}^{-1}\partial\mathbf{X}$ for some configuration $\mathbf{X}$. Then automatically $\mathrm{d}\boldsymbol{\xi} + \boldsymbol{\xi}\wedge\boldsymbol{\xi} = 0$. And conversely, when the Maurer–Cartan equation holds, one can locally reconstruct $\mathbf{X}$ such that $\boldsymbol{\xi} = \mathbf{X}^{-1}\partial\mathbf{X}$.

The Maurer–Cartan compatibility equation (111) can be written

$$\partial_i \boldsymbol{\xi}_k \;-\; \partial_k \boldsymbol{\xi}_i \;+\; [\boldsymbol{\xi}_i, \boldsymbol{\xi}_k] \;=\; 0\,, \tag{112}$$

where the term in brackets is the Lie bracket—the commutator. To compute it, substitute the block form (16) into it:

$$\begin{aligned}
[\boldsymbol{\xi}_i, \boldsymbol{\xi}_k] &= \boldsymbol{\xi}_i, \boldsymbol{\xi}_k \;-\; \boldsymbol{\xi}_k, \boldsymbol{\xi}_i \\
&= \begin{bmatrix} \boldsymbol{\Gamma}_i & \boldsymbol{\epsilon}_{,i} \\ 0 & 0 \end{bmatrix}\begin{bmatrix} \boldsymbol{\Gamma}_k & \boldsymbol{\epsilon}_{,k} \\ 0 & 0 \end{bmatrix} - \begin{bmatrix} \boldsymbol{\Gamma}_k & \boldsymbol{\epsilon}_{,k} \\ 0 & 0 \end{bmatrix}\begin{bmatrix} \boldsymbol{\Gamma}_i & \boldsymbol{\epsilon}_{,i} \\ 0 & 0 \end{bmatrix} = \begin{bmatrix} \boldsymbol{\Gamma}_i \boldsymbol{\Gamma}_k & \boldsymbol{\Gamma}_i \boldsymbol{\epsilon}_{,k} \\ 0 & 0 \end{bmatrix} - \begin{bmatrix} \boldsymbol{\Gamma}_k \boldsymbol{\Gamma}_i & \boldsymbol{\Gamma}_k \boldsymbol{\epsilon}_{,i} \\ 0 & 0 \end{bmatrix}
\end{aligned}$$

Therefore,

$$[\boldsymbol{\xi}_i, \boldsymbol{\xi}_k] = \begin{bmatrix} [\boldsymbol{\Gamma}_i, \boldsymbol{\Gamma}_k] & \boldsymbol{\Gamma}_i \boldsymbol{\epsilon}_{,k} - \boldsymbol{\Gamma}_k \boldsymbol{\epsilon}_{,i} \\ 0 & 0 \end{bmatrix}$$

Substituting this into (112) gives the Maurer–Cartan compatibility equation in the form

$$\begin{bmatrix} \partial_i \boldsymbol{\Gamma}_k - \partial_k \boldsymbol{\Gamma}_i + [\boldsymbol{\Gamma}_i, \boldsymbol{\Gamma}_k] & \boldsymbol{\epsilon}_{,k,i} - \boldsymbol{\epsilon}_{,i,k} + \boldsymbol{\Gamma}_i \boldsymbol{\epsilon}_{,k} - \boldsymbol{\Gamma}_k \boldsymbol{\epsilon}_{,i} \\ 0 & 0 \end{bmatrix} = \mathbf{0}$$

So this generates two blocks. The rotational block is

$$\partial_i \boldsymbol{\Gamma}_k \;-\; \partial_k \boldsymbol{\Gamma}_i \;+\; [\boldsymbol{\Gamma}_i, \boldsymbol{\Gamma}_k] \;=\; 0\,.$$

But we will focus only on the translational block:

$$\boldsymbol{\epsilon}_{,k,i} - \boldsymbol{\epsilon}_{,i,k} + \boldsymbol{\Gamma}_i \boldsymbol{\epsilon}_{,k} - \boldsymbol{\Gamma}_k \boldsymbol{\epsilon}_{,i} \;=\; 0\,, \tag{113}$$

or in index notation,

$$\epsilon_{p,k,i} - \epsilon_{p,i,k} + \Gamma_{pj,i}\, \epsilon_{j,k} - \Gamma_{pj,k}\, \epsilon_{j,i} \;=\; 0\,.$$

For small-strain Saint-Venant torsion, the Lie bracket terms are higher order, so we assume

$$\boldsymbol{\Gamma}_i \boldsymbol{\epsilon}_{,k} - \boldsymbol{\Gamma}_k \boldsymbol{\epsilon}_{,i} \;=\; 0\,,$$

which means that (113) simplifies to

$$\boldsymbol{\epsilon}_{,k,i} \;=\; \boldsymbol{\epsilon}_{,i,k}$$

For the axial displacement component, with cross-section directions given by $i = 2\,,\; k = 1\,,$ this becomes

$$\begin{aligned}
\epsilon_{3,12} &= \epsilon_{3,21} \\
\partial_y \epsilon_{3,1} &= \partial_x \epsilon_{3,2}\,.
\end{aligned} \tag{114}$$

To get an expression to use for the ϵ gradients, start with $\eta_{ki} = \Gamma_{kj,i} R_j + \epsilon_{k,i}$ in (37):

$$\begin{aligned}
\gamma_{13} &= \eta_{13} + \eta_{31} & \gamma_{23} &= \eta_{23} + \eta_{32} \\
&= \Gamma_{1j,3} R_j + \cancel{\epsilon_{1,3}} + \cancel{\Gamma_{3j,1}} R_j + \epsilon_{3,1} & &= \Gamma_{2j,3} R_j + \cancel{\epsilon_{2,3}} + \cancel{\Gamma_{3j,2}} R_j + \epsilon_{3,2}
\end{aligned} \tag{115}$$

For torsion about the z-axis, the rotational strain is

$$\boldsymbol{\Gamma}_{,3} = \begin{bmatrix} 0 & -\phi' & 0 \\ \phi' & 0 & 0 \\ 0 & 0 & 0 \end{bmatrix}.$$

Noting the nonzero components, we can simplify γ_{ik} to

$$\gamma_{13} = \Gamma_{12,3} R_2 + \epsilon_{3,1} = -\phi' y + \epsilon_{3,1} \qquad \gamma_{23} = \Gamma_{21,3} R_1 + \epsilon_{3,2} = \phi' x + \epsilon_{3,2} \tag{116}$$

Solve these for the ϵ gradients:

$$\epsilon_{3,1} = \gamma_{13} + \phi' y \qquad \epsilon_{3,2} = \gamma_{23} - \phi' x \tag{117}$$

and substitute them into the Maurer–Cartan compatibility condition (114):

$$\begin{aligned} \partial_y(\gamma_{13} + \phi' y) &= \partial_x(\gamma_{23} - \phi' x) \\ \gamma_{13,2} + \phi' &= \gamma_{23,1} - \phi' \\ \gamma_{13,2} - \gamma_{23,1} &= -2\phi' \end{aligned}$$

Using Hooke's law (49) gives

$$\sigma_{13,2} - \sigma_{23,1} = -2G\phi' ,$$

and using Prandtl's stress function from (107) gives

$$\begin{aligned} \varphi_{,22} + \varphi_{,11} &= -2G\phi' \\ \nabla^2\varphi &= -2G\phi' \end{aligned} \tag{118}$$

So we see that the classical compatibility equations are a special case of the more fundamental Maurer–Cartan equation (111). Notice that we again see a factor of 2 as we did in (110). The first one results from the divergence of the radial field, and the second results from the curl of the rotational field. The torque derivation uses (x, y), and the compatibility derivation uses $(-y, x)$. But the second is just the first rotated by 90°. So the common factor of 2 is not a coincidence.

Series Solution for φ

The rectangular cross-section requires that the Prandtl stress-function φ be written in the powerful form of a Fourier/Galerkin series (see, e.g., Ike 2024):

$$\varphi(x, y) = \sum_{m=1}^{N}\sum_{n=1}^{N} \varphi_{mn} = \sum_{m=1}^{N}\sum_{n=1}^{N} a_{mn} \cos\left(\frac{m\pi x}{W}\right)\cos\left(\frac{n\pi y}{H}\right), \quad \text{[N/m]} \tag{119}$$

where the coefficients are given by

$$a_{mn} = \frac{32G\phi'}{\pi^4} \frac{\sin(m\pi/2)\sin(n\pi/2)}{mn[(m/W)^2 + (n/H)^2]}. \quad \text{[N/m]} \tag{120}$$

As $N \to \infty$, the series becomes exact. Notice that when n or m are even, the coefficients vanish. Notice also that a_{mn}, and hence the entire field, are proportional to the twist rate ϕ'.

Write (110) for a single mode

$$\begin{aligned} M_{mn} &= 2\int_A \varphi_{mn}\,\mathrm{d}A \\ &= 2a_{mn}\int_{-W/2}^{W/2} \cos\left(\frac{m\pi x}{W}\right)\mathrm{d}A \int_{-H/2}^{H/2} \cos\left(\frac{n\pi y}{H}\right)\mathrm{d}A \end{aligned}$$

Integrating that mode gives

$$M_{mn} \;=\; 8a_{mn}\frac{WH}{mn\pi^2}\sin\left(\frac{m\pi}{2}\right)\sin\left(\frac{n\pi}{2}\right).$$

Summing over all modes as required by (119) then gives

$$M \;=\; 8\frac{WH}{\pi^2}\sum_{m=1}^{N}\sum_{n=1}^{N}\frac{a_{mn}}{mn}\sin\left(\frac{m\pi}{2}\right)\sin\left(\frac{n\pi}{2}\right). \tag{121}$$

We could also substitute the coefficient (120) into (121) and write

$$M \;=\; G\phi'\left[\frac{WH}{\pi^6}\sum_{m=1}^{N}\sum_{n=1}^{N}256\frac{\sin^2(m\pi/2)\sin^2(n\pi/2)}{m^2n^2[(m/W)^2+(n/H)^2]}\right] \tag{122}$$

The quantity in square brackets we define as J, the effective polar moment of inertia of the rectangular cross-section, which is a generalization of I in (93) for the circular shaft. Then

$$M \;=\; G\,\phi'\,J\,. \tag{123}$$

So the series has produced J, and the applied torque M will determine the twist rate ϕ'.

For the rubber block of this example, the series yields, with $N = 51$,

$$J \;=\; 9.1821\times10^{-8} + 4.8503\times10^{-9} + 8.521\times10^{-10} + ... \;=\; 10.143\times10^{-8}\,\mathrm{m}^4\,. \tag{124}$$

We can compare this with the value predicted by the standard approximation (Young and Budynas 2002):

$$\begin{aligned} J \;&=\; HW^3\left[\frac{1}{3} - 0.21\frac{W}{H}\left[1-\frac{1}{12}\left(\frac{W}{H}\right)^4\right]\right] \qquad \text{for } a \geq b \\ &=\; 9.9805\times10^{-8}\,\mathrm{m}^4 \end{aligned}$$

which is within 2%.

Then, with $G = 10\,\mathrm{MPa}$ for the rubber block of this example, (123) gives the twist rate

$$\begin{aligned} \phi' \;&=\; \frac{M_z}{G\,J} \;=\; \frac{5\ \mathrm{Nm}}{10\,\mathrm{MPa}\ (10.143\times10^{-8}\,\mathrm{m}^4)} \\ &=\; 4.93\ \mathrm{rad/m}. \end{aligned}$$

We can compute the stress field by using (107) and computing the needed derivatives $\varphi_{,1}$ and $\varphi_{,2}$ using (119). This gives

$$\sigma_{13} \;=\; \varphi_{,2} \;=\; -\sum_{m=1}^{N}\sum_{n=1}^{N}\frac{n\pi}{H}a_{mn}\cos\left(\frac{m\pi x}{W}\right)\sin\left(\frac{n\pi y}{H}\right) \tag{125}$$

$$\sigma_{23} \;=\; -\,\varphi_{,1} \;=\; \sum_{m=1}^{N}\sum_{n=1}^{N}\frac{m\pi}{W}a_{mn}\sin\left(\frac{m\pi x}{W}\right)\cos\left(\frac{n\pi y}{H}\right). \tag{126}$$

The torsional shear stress magnitude

$$\tau = \sqrt{{\sigma_{13}}^2 + {\sigma_{23}}^2} \tag{127}$$

is plotted in Figure 3 using a spreadsheet.

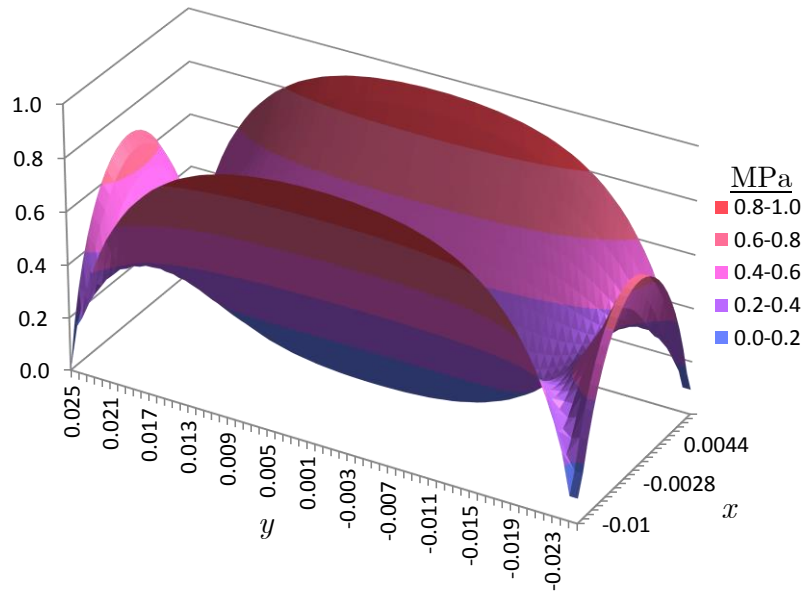

Figure 3. Torsional stress (127) in the mid-span ($z = 0.1\,\mathrm{m}$) section of rubber block.

Cross-Section Warping

Torsion causes warping (axial strain) in non-circular sections in order to satisfy the closure condition $\mathrm{d}\omega_3 = 0$ in (72). This appears as non-uniform axial strain at a given cross section. To find the warping of the cross-section, substitute Hooke's law (49) into (117) again

$$\epsilon_{3,1} \;=\; \frac{\sigma_{13}}{G} + \phi' y \qquad\qquad \epsilon_{3,2} \;=\; \frac{\sigma_{23}}{G} - \phi' x\,, \tag{128}$$

followed by Prandtl's stress function (107):

$$\epsilon_{3,1} \;=\; \phi' y + \frac{\varphi_{,2}}{G} \qquad\qquad \epsilon_{3,2} \;=\; -\,\phi' x - \frac{\varphi_{,1}}{G}\,. \tag{129}$$

The compatibility equation (118) ensures that these two gradients integrate to a single ϵ_3. But we can, if we wish, define the warping function ψ

$$\phi'(z)\,\psi(x,y) \;=\; \epsilon_3 \tag{130}$$

so that

$$\psi_{,1} \;=\; y \;+\; \frac{\varphi_{,2}}{G\phi'} \qquad\qquad \psi_{,2} \;=\; -\,x \;-\; \frac{\varphi_{,1}}{G\phi'}\,,$$

but it is not necessary. Incidentally, differentiating these again gives identities:

$$\psi_{,11} \;=\; \frac{\varphi_{,21}}{G\phi'} \qquad\qquad \psi_{,22} \;=\; -\,\frac{\varphi_{,12}}{G\phi'}$$

that show that the warping function is harmonic since:

$$\psi_{,11} \;+\; \psi_{,22} \;=\; 0\,.$$

Now differentiate (119) as needed to substitute into (129), and integrate to get

$$\epsilon_3^{(\mathrm{w})} \;=\; \phi' xy \;-\; \sum_{mn=0}^{\infty} \frac{a_{mn}}{G}\,\frac{n}{m}\,\frac{W}{H}\sin\!\left(\frac{m\pi x}{W}\right)\sin\!\left(\frac{n\pi y}{H}\right) \;+\; f(z)\,, \tag{131}$$

The two equations of (129) show that the integration constant f is not a function of x or y. For example, for the corner point $r = [0.01, 0.025, 0.1]$ in the cross-section of the rubber block, this series, with $N = 51$, yields an axial warping displacement [neglecting axial compression $f(z)$] of

$$\epsilon_3^{(\mathrm{w})} \;=\; 0.70\,\mathrm{mm}.$$

Notice that the warping is not imposed using an external moment arm. It appears as the minimizing translational Maurer–Cartan component. The axial strain of (131) is shown in Figure 4. For axial warping in pure torsion with constant twist rate ϕ' such as this example, the gradient of (130) becomes

$$\nabla \boldsymbol{\epsilon}^{(\mathrm{w})} = \begin{bmatrix} \phi'\,\psi_{,x} \\ \phi'\,\psi_{,y} \\ 0 \end{bmatrix} \qquad\qquad \text{(warping)}$$

The fact that $\epsilon_{3,3}^{(\mathrm{w})} = 0$ affirms that the amount of axial warping is independent of z.

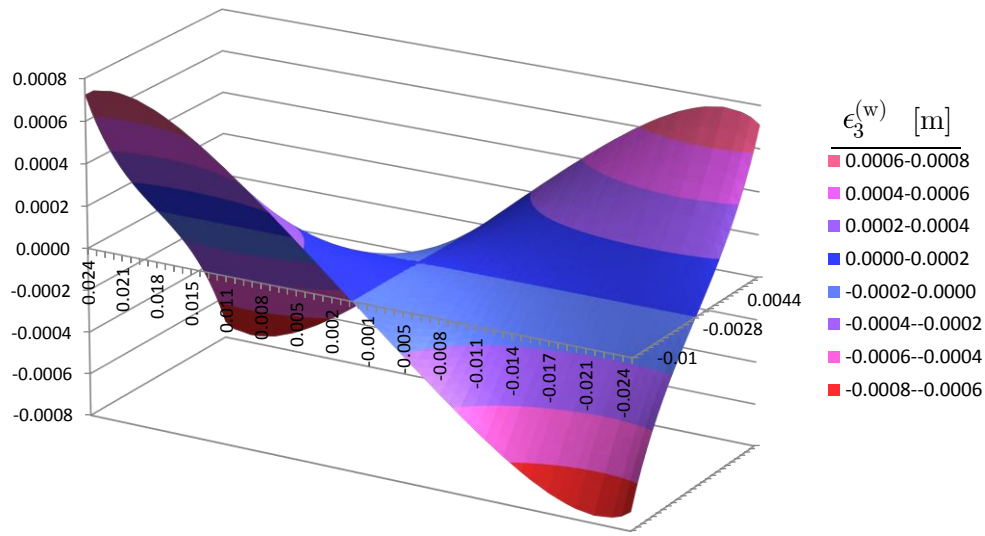

Figure 4. Axial displacement due to torsional warping of the rubber block (all units in m).

Summary of Combined Loading

Bending about $\mathbf{e}_1$

$$\boldsymbol{\Gamma}_{,3} = \begin{bmatrix} 0 & 0 & 0 \\ 0 & 0 & -\kappa_x \\ 0 & \kappa_x & 0 \end{bmatrix}$$

$$\boldsymbol{\eta}_{,3} = \boldsymbol{\Gamma}_{,3}\cdot\mathbf{R} \;=\; \begin{bmatrix} 0 \\ 0 \\ \kappa_x\, y \end{bmatrix}$$

Bending about $\mathbf{e}_2$

$$\boldsymbol{\Gamma}_{,3} = \begin{bmatrix} 0 & 0 & \kappa_y \\ 0 & 0 & 0 \\ -\kappa_y & 0 & 0 \end{bmatrix}$$

$$\boldsymbol{\eta}_{,3} = \boldsymbol{\Gamma}_{,3}\cdot\mathbf{R} \;=\; \begin{bmatrix} 0 \\ 0 \\ -\kappa_y\, x \end{bmatrix}$$

Torsion about $\mathbf{e}_3$

$$\boldsymbol{\Gamma}_{,3} = \begin{bmatrix} 0 & -\phi' & 0 \\ \phi' & 0 & 0 \\ 0 & 0 & 0 \end{bmatrix} \qquad \begin{aligned} \epsilon_{3,1} &= \phi'\psi_{,x} \\ \epsilon_{3,2} &= \phi'\psi_{,y} \end{aligned}$$

$$\boldsymbol{\gamma}_{\bullet 3} = \boldsymbol{\Gamma}_{,3}\cdot\mathbf{R} + \boldsymbol{\epsilon}_{3,i} = \phi' \begin{bmatrix} -y \\ x \\ 0 \end{bmatrix} + \begin{bmatrix} \epsilon_{3,1}^{(\mathrm{w})} \\ \epsilon_{3,2}^{(\mathrm{w})} \\ 0 \end{bmatrix}$$

$$\boldsymbol{\eta} = \boldsymbol{\Gamma}\cdot\mathbf{R} = \begin{bmatrix} 0 & 0 & 0 \\ 0 & 0 & 0 \\ 0 & \eta_{32} & \kappa_x\, y \end{bmatrix} \quad \boldsymbol{\eta} = \boldsymbol{\Gamma}\cdot\mathbf{R} = \begin{bmatrix} 0 & 0 & 0 \\ 0 & 0 & 0 \\ \eta_{31} & 0 & -\kappa_y x \end{bmatrix} \qquad \boldsymbol{\eta} = \boldsymbol{\Gamma}\cdot\mathbf{R} = \begin{bmatrix} 0 & 0 & -\phi'\, y \\ 0 & 0 & \phi'\, x \\ 0 & 0 & 0 \end{bmatrix}$$

A summary of the values, with no bending about the y-axis, is as follows:

$$\Gamma_{1j,3}R_j \;=\; \Gamma_{12,3}R_2 \;=\; -\,\phi' y \tag{132}$$

$$\Gamma_{2j,3}R_j \;=\; \Gamma_{21,3}R_1 \;=\; \phi' x \tag{133}$$

$$\Gamma_{3j,3}R_j \;=\; \Gamma_{32,3}R_2 \;=\; \kappa_x\, y \tag{134}$$

$$\epsilon_{3,1} = \epsilon_{3,1}^{(\mathrm{w})} \qquad \text{[from (131)]}$$

$$\epsilon_{3,2} \;=\; \epsilon_{3,2}^{(\mathrm{w})} \;+\; \frac{E}{2G}\kappa_x'\left(\frac{H^2}{4} - y^2\right) \qquad \text{[from (131)]}$$

$$\epsilon_{3,3} = F\,/\,(EA)$$

Then the η values are

$$\eta_{13} \;=\; \Gamma_{12,3}R_2 \;+\; \cancel{\epsilon_{1,3}} \;=\; -\,\phi' y$$

$$\eta_{23} \;=\; \Gamma_{21,3}R_1 \;+\; \cancel{\epsilon_{2,3}} \;=\; \phi' x$$

$$\eta_{33} \;=\; \Gamma_{3j,3}R_j \;+\; \epsilon_{33} \;=\; \kappa_x\, y \;+\; F/(EA) \tag{135}$$

$$\eta_{31} \;=\; \cancel{\Gamma_{3j,1}R_j} \;+\; \epsilon_{3,1} \;=\; \epsilon_{3,1}^{(\mathrm{w})}$$

$$\eta_{32} \;=\; \cancel{\Gamma_{3j,2}R_j} \;+\; \epsilon_{3,2} \;=\; \epsilon_{3,2}^{(\mathrm{w})} \;+\; \frac{E}{2G}\kappa_x'\left(\frac{H^2}{4} - y^2\right) \tag{136}$$

$$\gamma_{13} \;=\; (\eta_{13} + \eta_{31}) \;=\; -\,\phi' y \;+\; \epsilon_{3,1}^{(\mathrm{w})} \tag{137}$$

$$\gamma_{23} \;=\; (\eta_{23} + \eta_{32}) \;=\; \Gamma_{2j,3}R_j \;+\; \cancel{\epsilon_{2,3}} \;+\; \cancel{\Gamma_{3j,2}}R_j + \epsilon_{3,2}^{(\mathrm{w})}$$

$$\;=\; \phi' x \;+\; \epsilon_{3,2}^{(\mathrm{w})} \;+\; \frac{E}{2G}\kappa_x'\left(\frac{H^2}{4} - y^2\right) \tag{138}$$

Combining all these modes together, we obtain

$$\boldsymbol{\eta} \;=\; (\boldsymbol{\Gamma}\cdot\mathbf{R} \;+\; \boldsymbol{\epsilon}) \;=\; \begin{bmatrix} 0 & 0 & -\phi'\, y \\ 0 & 0 & \phi'\, x \\ 0 & 0 & \kappa_x\, y \end{bmatrix} + \begin{bmatrix} 0 & 0 & 0 \\ 0 & 0 & 0 \\ \epsilon_{3,1}^{(\mathrm{w})} & \epsilon_{3,2}^{(\mathrm{w})} + \dfrac{E}{2G}\kappa_x'\left(\dfrac{H^2}{4} - y^2\right) & F/(EA) \end{bmatrix}. \tag{139}$$

Constitutive Relation

The local strain energy density is, according to (38),

$$w \;=\; \frac{1}{2}E{\eta_{33}}^2 \;+\; \frac{1}{2}G\,(\eta_{13} + \eta_{31})^2 \;+\; \frac{1}{2}G\,(\eta_{23} + \eta_{32})^2\,.$$

By referring to the curvature matrices Γ above, we can immediately write

$$w \;=\; \frac{1}{2}E\,(\Gamma_{3j,3}R_j + \epsilon_{3,3})^2 \;+\; \frac{1}{2}G\,(\Gamma_{1j,3}R_j + \cancel{\epsilon_{1,3}} + \cancel{\Gamma_{3j,1}}R_j + \epsilon_{3,1})^2 \\ +\; \frac{1}{2}G\,(\Gamma_{2j,3}R_j + \cancel{\epsilon_{2,3}} + \cancel{\Gamma_{3j,2}}R_j + \epsilon_{3,2})^2 \tag{140}$$

Moments

For moments, take the derivative $\partial w/\partial \mathbf{\Gamma}_{,3}$:

$$\boldsymbol{\mu}_{,3} \;=\; \frac{\partial w}{\partial \mathbf{\Gamma}_{,3}} \;=\; \mu_{pq,3}\,\mathbf{e}_p\,\mathbf{e}_q\,\mathbf{e}_3\,,$$

where, from (57),

$$\mu_{3q,3} \;=\; \frac{\partial w}{\partial \Gamma_{3q,3}} \;=\; E\,\eta_{33}\,R_q\,, \tag{141}$$

when $p = r$. And when $p \neq r$,

$$\mu_{pq,3} \;=\; \frac{\partial w}{\partial \Gamma_{pq,3}} \;=\; G\,(\eta_{p3} + \eta_{3p})\,R_q \;=\; G\,[(\Gamma_{pj,3}R_j + \epsilon_{p,3}) + (\Gamma_{3j,p}R_j + \epsilon_{3,p})]\,R_q\,. \tag{142}$$

For (141), with $q = 1$,

$$\mu_{31,3} \;=\; \frac{\partial w}{\partial \Gamma_{31,3}} \;=\; E\,(\Gamma_{3j,3}R_j + \epsilon_{3,3})\,R_1 \\ =\; E\,(\Gamma_{31,3}R_1 + \Gamma_{32,3}R_2 + \epsilon_{3,3})\,R_1$$

Substituting in values from (99) gives

$$\mu_{31,3} \;=\; E\,(-\kappa_y x + \kappa_x y + \epsilon_{3,3})\,x\,,$$

and with $q = 2$,

$$\mu_{32,3} \;=\; E\,(-\kappa_y x + \kappa_x y + \epsilon_{3,3})\,y\,.$$

For (142), with $p = 1$,

$$\mu_{1q,3} \;=\; \frac{\partial w}{\partial \Gamma_{1q,3}} \;=\; G\,[(\Gamma_{1j,3}R_j + \cancel{\epsilon_{1,3}}) + (\cancel{\Gamma_{3j,1}}R_j + \epsilon_{3,1})]\,R_q$$

For $q = 1$, we refer to (132) and write (142) as

$$\mu_{11,3} \;=\; \frac{\partial w}{\partial \Gamma_{11,3}} \;=\; G\,(\cancel{\Gamma_{11,3}}R_1 + \Gamma_{12,3}R_2 + \epsilon_{3,1})\,R_1 \\ =\; G\,(-\phi' y \;+\; \epsilon_{3,1}^{(\mathrm{w})})\,x$$

For $q = 2$, (142) becomes

$$\mu_{12,3} \;=\; \frac{\partial w}{\partial \Gamma_{12,3}} \;=\; G\,(\Gamma_{12,3}R_2 + \epsilon_{3,1})\,R_2 \\ =\; G\,(-\phi' y \;+\; \epsilon_{3,1}^{(\mathrm{w})})\,y$$

With $p = 2$ in (142), we obtain

$$\mu_{2q,3} = \frac{\partial w}{\partial \Gamma_{2q,3}} = G[(\Gamma_{21,3}R_1 + \cancel{\Gamma_{22,3}}R_2 + \cancel{\epsilon_{2,3}}) + (\cancel{\Gamma_{3j,2}}R_j + \epsilon_{3,2})]\,R_q$$

Referring to (138), with $q = 1$,

$$\mu_{21,3} = \frac{\partial w}{\partial \Gamma_{21,3}} = G(\Gamma_{21,3}R_1 + \epsilon_{3,2})\,R_1$$

$$= G\left[\phi' x + \epsilon_{3,2}^{(\mathrm{w})} + \frac{E}{2G}\kappa_x'\left(\frac{H^2}{4} - y^2\right)\right]x$$

and with $q = 2$,

$$\mu_{22,3} = \frac{\partial w}{\partial \Gamma_{22,3}} = G(\Gamma_{21,3}R_1 + \epsilon_{3,2})\,R_2$$

$$= G\left[\phi' x + \epsilon_{3,2}^{(\mathrm{w})} + \frac{E}{2G}\kappa_x'\left(\frac{H^2}{4} - y^2\right)\right]y$$

We need not check the case with $p = 3$ because that case was already done with the normal strain gradient (since $r = 3$ throughout).

We have now collected all the terms for the expansion

$$\boldsymbol{\mu}_{,3} = \mu_{11,3}\,\mathbf{e}_1\,\mathbf{e}_1\,\mathbf{e}_3 + \mu_{12,3}\,\mathbf{e}_1\,\mathbf{e}_2\,\mathbf{e}_3 + \mu_{21,3}\,\mathbf{e}_2\,\mathbf{e}_1\,\mathbf{e}_3 + \mu_{22,3}\,\mathbf{e}_2\,\mathbf{e}_2\,\mathbf{e}_3 + \mu_{31,3}\,\mathbf{e}_3\,\mathbf{e}_1\,\mathbf{e}_3 + \mu_{32,3}\,\mathbf{e}_3\,\mathbf{e}_2\,\mathbf{e}_3$$

Substituting the above values gives

$$\boldsymbol{\mu}_{,3} = G(\epsilon_{3,1}^{(\mathrm{w})} - \phi' y)x\,\mathbf{e}_3 + G(\epsilon_{3,1}^{(\mathrm{w})} - \phi' y)y\,\mathbf{e}_1\,\mathbf{e}_2\,\mathbf{e}_3 + G\left[(\phi' x + \epsilon_{3,2}^{(\mathrm{w})}) + \frac{E}{2G}\kappa_x'\left(\frac{H^2}{4} - y^2\right)\right]x\,\mathbf{e}_2\,\mathbf{e}_1\,\mathbf{e}_3$$
$$+ G\left[(\phi' x + \epsilon_{3,2}^{(\mathrm{w})}) + \frac{E}{2G}\kappa_x'\left(\frac{H^2}{4} - y^2\right)\right]y\,\mathbf{e}_3 + E(-\kappa_y x + \kappa_x y + \epsilon_{3,3})\,x\,\mathbf{e}_3\,\mathbf{e}_1\,\mathbf{e}_3$$
$$+ E(-\kappa_y x + \kappa_x y + \epsilon_{3,3})\,y\,\mathbf{e}_3\,\mathbf{e}_2\,\mathbf{e}_3$$

Permuting some pairs of the basis vectors and noting that $\mathbf{e}_i\mathbf{e}_i = 1$ gives

$$\boldsymbol{\mu}_{,3} = G\left[\epsilon_{3,1}^{(\mathrm{w})}x + \epsilon_{3,2}^{(\mathrm{w})}y + \frac{E}{2G}\kappa_x'\left(\frac{H^2}{4} - y^2\right)y\right]\mathbf{e}_3$$
$$+ G\left\{(\epsilon_{3,1}^{(\mathrm{w})} - \phi' y)y - \left[(\phi' x + \epsilon_{3,2}^{(\mathrm{w})}) + \frac{E}{2G}\kappa_x'\left(\frac{H^2}{4} - y^2\right)\right]x\right\}\mathbf{e}_1\mathbf{e}_2\mathbf{e}_3$$
$$+ E(\kappa_y x^2 - \kappa_x xy - \epsilon_{3,3}x)\,\mathbf{e}_1 + E(\kappa_y xy - \kappa_x y^2 - \epsilon_{3,3}y)\mathbf{e}_2$$

The interesting aspect of this expression is that torsion (before plane selection) has become a trivector, the bending parts have become vectors, and the compression vanishes from the moment object. So the torsion and bending are being separated by grade, not by introducing separate constitutive laws. The tensor $\mu_{kj,i}$ appears to be the coordinate representation of a geometric object whose vector grades encode bending-like effects and whose trivector grades encode torsional effects. This suggests that the resultants in $\boldsymbol{\mu} = \mu_{pq,r}\mathbf{e}_p\mathbf{e}_q\mathbf{e}_r$ can be classified by grade.

With bending only about the x-axis as in the present example, $\kappa_y = 0$, so

$$\begin{aligned}\boldsymbol{\mu}_{,3} \;=\; & G\left[\epsilon_{3,1}^{(\mathrm{w})} x + \epsilon_{3,2}^{(\mathrm{w})} y + \frac{E}{2G}\kappa_x'\left(\frac{H^2}{4} - y^2\right) y\right]\mathbf{e}_3 \\ & + G\left\{(\epsilon_{3,1}^{(\mathrm{w})} - \phi' y) y - \left[(\phi' x + \epsilon_{3,2}^{(\mathrm{w})}) + \frac{E}{2G}\kappa_x'\left(\frac{H^2}{4} - y^2\right)\right] x\right\}\mathbf{e}_1\mathbf{e}_2\mathbf{e}_3 \\ & - E(\kappa_x xy + \epsilon_{3,3} x)\mathbf{e}_1 \;-\; E(\kappa_x y^2 + \epsilon_{3,3} y)\mathbf{e}_2\end{aligned} \tag{143}$$

To compute the moments due to bending (or, more likely, to solve for the curvature κ_x based on the known moment), we extract the vectors of the above relation:

$$\begin{aligned}\mathbf{M} \;=\; & \int_A G\left[\epsilon_{3,1}^{(\mathrm{w})} x + \epsilon_{3,2}^{(\mathrm{w})} y + \frac{E}{2G}\kappa_x'\left(\frac{H^2}{4} - y^2\right) y\right]\mathbf{e}_3\,\mathrm{d}\mathbf{A} \\ & - \int_A E(\kappa_x xy + \epsilon_{3,3} x)\mathbf{e}_1\,\mathrm{d}\mathbf{A} \;-\; \int_A E(\kappa_x y^2 + \epsilon_{3,3} y)\mathbf{e}_2\,\mathrm{d}\mathbf{A}\end{aligned}$$

Since the domain of integration for the rectangular section is symmetrical, all these terms integrate out to zero except the term with y^2. So

$$\mathbf{M} \;=\; -\int_A E\,\kappa_x y^2\,\mathbf{e}_2\,\mathbf{e}_3\,\mathrm{d}A\,.$$

The three terms that vanished would not have vanished if $\mathbf{R}$ were measured from a non-centroidal point or perhaps if the axial compression were applied off center.

The magnitude of the moment is then

$$M \;=\; E\,\kappa_x(z)\int_A y^2\mathrm{d}A \;=\; E\,\kappa_x(z)\int_{-W/2}^{W/2}\int_{-H/2}^{H/2} y^2\mathrm{d}y\,\mathrm{d}x \;=\; E\,\kappa_x(z)\frac{WH^3}{12} \tag{144}$$

Solving for curvature gives

$$\kappa_x(z) \;=\; \frac{M(z)}{E\int_A y^2\mathrm{d}A} \;=\; \frac{F_y\,(L-z)}{E\,I_x}\,. \tag{145}$$

To compute the moments due to torsion (or rather compute the associated curvature), we extract the trivectors of (143):

$$\mathbf{M} \;=\; -G\phi'\int_A\left[-\frac{\epsilon_{3,1}^{(\mathrm{w})}}{\phi'}y + y^2 + x^2 + \frac{\epsilon_{3,2}^{(\mathrm{w})}}{\phi'}x \;+\; \frac{E}{2G}\frac{\kappa_x'}{\phi'}x\left(\frac{H^2}{4} - y^2\right)\right]\mathbf{e}_1\,\mathbf{e}_2\,\mathbf{e}_3\,\mathrm{d}\mathbf{A} \tag{146}$$

The integral is

$$J \;=\; \int_A\left[x^2 + y^2 - \frac{1}{\phi'}(\epsilon_{3,1}^{(\mathrm{w})} y - \epsilon_{3,2}^{(\mathrm{w})} x) \;+\; \frac{E}{2G}\frac{\kappa_x'}{\phi'}x\left(\frac{H^2}{4} - y^2\right)\right]\mathrm{d}A,$$

so we can write the magnitude of (146) as

$$M \;=\; G\,\phi'\,J\,.$$

Note how this J for this non-circular cross-section under a combined bending load differs from that in (93) for the circular cylinder in pure torsion.

Having obtained the sectional moments by integrating the rotational contributions of the constitutive law over the cross-section, attention now turns to the force resultants.

Forces

Whereas the moment expressions were weighted by the position vector within the section, the force expressions depend directly on the translational strain components. Together, these two sets of resultants completely characterize the internal loading carried by the beam section. For forces, take the derivative $\partial w/\partial \boldsymbol{\epsilon}$, where w is given by (140). The normal force is found by substituting (135) into (51):

$$\omega_3 \;=\; \int_A E\,\eta_{33}\,\mathrm{d}A \;=\; E\int_A (\kappa_x\, y \;+\; F/(EA))\,\mathrm{d}A\,.$$

The shear forces in the section are found by substituting (137) and (138) into (52):

$$\omega_1 \;=\; G\int_A \gamma_{13}\,\mathrm{d}A \;=\; G\int_A (\epsilon_{3,1}^{(\mathrm{w})} - \phi' y)\,\mathrm{d}A$$

$$\omega_2 \;=\; G\int_A \gamma_{23}\,\mathrm{d}A \;=\; G\int_A \left[\phi' x \;+\; \epsilon_{3,2}^{(\mathrm{w})} \;+\; \frac{E}{2G}\kappa_x'\left(\frac{H^2}{4} - y^2\right)\right]\mathrm{d}A$$

With the rotational and translational resultants now established, the intrinsic constitutive description of the beam section is complete. The remaining task is the displacement field and reconstruction of the corresponding beam configuration from computed strain measures.

<u>Bending Displacement</u>

The first displacement check that can be done is to compare with the classical formula for the deflection of a cantilever beam. The curvature κ_x was computed in (145) for bending about the x-axis. The bending angle β is the integral of curvature in the z direction:

$$\beta(z) \;=\; \int_0^z \kappa_x(s)\mathrm{d}s \;=\; \frac{F_y}{E\int y^2\mathrm{d}A}\int_0^z (L-s)\mathrm{d}s$$

$$= \frac{F_y}{E\int y^2\mathrm{d}A}\left(Lz - \frac{z^2}{2}\right) \tag{147}$$

This is the exact accumulated rotation due to bending. The bending angle at the tip is found by evaluating it at $z = L$. This gives

$$\beta(L) \;=\; \frac{F_y L^2}{2EI_x}$$

For this case, we have already computed I_x in (144) to be $I_x = 2.0833\times10^{-7}\mathrm{m}^4$ so that with a bending force of 30 N as in this example, the bending angle at the tip is

$$\beta(L) \;=\; 0.096 \text{ rad.}$$

And if we want the deflection of the beam at the tip, we can integrate the angle β in (147) along the beam:

$$\delta(z) \;=\; \int_0^z \beta(s)\,\mathrm{d}s \;=\; \int_0^L \frac{F_y}{E\,I_y}\left(Ls - \frac{s^2}{2}\right)\mathrm{d}s \;=\; \frac{F_y L^3}{3E\,I_x}$$

which is the well-known formula for the deflection of a cantilever beam.

2.5. Reconstructing the Body from Strains

The intrinsic strain field $\boldsymbol{\xi}_i$ determines the configuration of the body via reconstruction. To distinguish this intrinsic strain from the resulting physical deformation of the material, the dimensional physical strain between neighboring material points will be defined. Then, the displacements will be found by integrating the strain gradient along z.

Start with (5)

$$\mathbf{p} = \boldsymbol{\Theta}\,\mathbf{r} + \mathbf{a}\,. \tag{148}$$

To define physical strain at, say, Point 1, first define the displacement vector between its transported position $\mathbf{p}_1$ and the same point $\mathbf{r}_1$ in the body before any load is applied. This displacement vector is given by

$$\boldsymbol{\zeta}_1 = \mathbf{p}_1 - \mathbf{r}_1\,.$$

However, the magnitude of this displacement does not, by itself, indicate the physical strain near Point 1 since the point may have been transported by rigid-body motion or by deformation elsewhere in the body. Local physical strain occurs when this displacement differs from that at a neighboring point, as follows:

$$\boldsymbol{\zeta}_2 - \boldsymbol{\zeta}_1 = (\mathbf{p}_2 - \mathbf{r}_2) - (\mathbf{p}_1 - \mathbf{r}_1)\,.$$

In differential form, physical strain can be written

$$\mathrm{d}\boldsymbol{\zeta} = \mathrm{d}\mathbf{p} - \mathrm{d}\mathbf{r}\,. \tag{149}$$

This is the local change in relative position of neighboring material points.

First, write $\mathrm{d}\mathbf{p}$ by differentiating (148):

$$\mathrm{d}\mathbf{p} = (\partial_i\boldsymbol{\Theta}\,\mathbf{r} + \boldsymbol{\Theta}\,\partial_i\mathbf{r} + \partial_i\mathbf{a})\mathrm{d}x_i$$

Use (28) and (30) to write

$$\mathrm{d}\mathbf{p} = \boldsymbol{\Theta}[\boldsymbol{\Gamma}_i\cdot\mathbf{r} + \frac{\partial\overline{\mathbf{r}}}{\partial x_i} + \boldsymbol{\epsilon}_{,i}]\mathrm{d}x_i \tag{150}$$

Most of the information can be gained by reconstructing cross-sections along the z direction; therefore, we take the following special case:

$$\mathrm{d}\mathbf{p} = \boldsymbol{\Theta}[\boldsymbol{\Gamma}_z\cdot\mathbf{r} + \frac{\partial\overline{\mathbf{r}}}{\partial z} + \boldsymbol{\epsilon}_{,z}]\mathrm{d}z\,. \tag{151}$$

So according to (149), physical strain is

$$\mathrm{d}\boldsymbol{\zeta} = \boldsymbol{\Theta}[\boldsymbol{\Gamma}_z\cdot\mathbf{r} + \frac{\partial\overline{\mathbf{r}}}{\partial z} + \boldsymbol{\epsilon}_{,z}]\mathrm{d}z - \mathrm{d}\mathbf{r}\,.$$

The integration for $\boldsymbol{\zeta}$ will be long but is entirely doable, and once done, it can be interrogated quickly and easily to examine various load cases without using FEA code.

The components of $\boldsymbol{\xi}_i$ are as follows for the rubber block in combined load:

$$\boldsymbol{\xi}_1 = \begin{bmatrix} 0 & 0 & 0 & 0 \\ 0 & 0 & 0 & 0 \\ 0 & 0 & 0 & \epsilon_{3,1} \\ 0 & 0 & 0 & 0 \end{bmatrix} \qquad \boldsymbol{\xi}_2 = \begin{bmatrix} 0 & 0 & 0 & 0 \\ 0 & 0 & 0 & 0 \\ 0 & 0 & 0 & \epsilon_{3,2} \\ 0 & 0 & 0 & 0 \end{bmatrix} \qquad \boldsymbol{\xi}_3 = \begin{bmatrix} 0 & -\phi' & 0 & 0 \\ \phi' & 0 & \kappa_x & 0 \\ 0 & -\kappa_x & 0 & \epsilon_{3,3} \\ 0 & 0 & 0 & 0 \end{bmatrix}$$

The nonzero elements in $\boldsymbol{\xi}_1$ and $\boldsymbol{\xi}_2$ arise from warping of the cross section due to torsion. Rather than integrate (150) over x and y, the easiest way to account for these is to simply add these axial strains to ϵ_{33} so that warping becomes part of the transported strain field.

<u>Displacements for the Combined Loading Example (Example 3)</u>

The combined rotation matrix for Example 3 is

$$\boldsymbol{\Theta}(z) = \boldsymbol{\Theta}_T(z)\boldsymbol{\Theta}_B(z)\,, \tag{152}$$

where

$$\boldsymbol{\Theta}_T = \begin{bmatrix} \cos\phi & -\sin\phi & 0 \\ \sin\phi & \cos\phi & 0 \\ 0 & 0 & 1 \end{bmatrix} \qquad \boldsymbol{\Theta}_B = \begin{bmatrix} 1 & 0 & 0 \\ 0 & \cos\beta & -\sin\beta \\ 0 & \sin\beta & \cos\beta \end{bmatrix}.$$

Since the rotational matrices $\boldsymbol{\Theta}_T(z)$ and $\boldsymbol{\Theta}_B(z)$ in (152) do not commute, we must decide on the load order, or else solve with a simultaneous assumption. The easiest way may be to allow bending first, then torsion. Doing this puts (152) into the form

$$\boldsymbol{\Theta}(z) = \begin{bmatrix} \cos\phi & -\sin\phi\cos\beta & \sin\phi\sin\beta \\ \sin\phi & \cos\phi\cos\beta & -\cos\phi\sin\beta \\ 0 & \sin\beta & \cos\beta \end{bmatrix}.$$

This rotation matrix is used in the integral of (151):

$$\boldsymbol{\zeta}(z,R) = \int_0^z \boldsymbol{\Theta}[\boldsymbol{\Gamma}_z \cdot \mathbf{r} + \frac{\partial \overline{\mathbf{r}}}{\partial z} + \boldsymbol{\epsilon}_{,z}]\,\mathrm{d}z - (\mathbf{r} - \mathbf{r}_0)\,, \tag{153}$$

where the constant of integration is

$$\mathbf{r} - \mathbf{r}_0 = \begin{bmatrix} x - x_0 \\ y - y_0 \\ z - z_0 \end{bmatrix} = \begin{bmatrix} 0 \\ 0 \\ z - 0 \end{bmatrix}$$

since integration is only in the z direction while x and y remain fixed during integration.

The combined curvature matrix is

$$\boldsymbol{\Gamma}_{,3} = \begin{bmatrix} 0 & -\phi' & 0 \\ \phi' & 0 & -\kappa_x \\ 0 & \kappa_x & 0 \end{bmatrix}.$$

Therefore,

$$\boldsymbol{\Gamma}_{,3} \cdot \mathbf{r} = \begin{bmatrix} -\phi' y \\ \phi' x - \kappa_x z \\ \kappa_x y \end{bmatrix} \quad \text{and} \quad \boldsymbol{\epsilon}_{,3} = \begin{bmatrix} 0 \\ 0 \\ \epsilon_{3,3} \end{bmatrix}.$$

Then

$$[\mathbf{\Gamma}_z \cdot \mathbf{r} + \frac{\partial \overline{\mathbf{r}}}{\partial z} + \boldsymbol{\epsilon}_{,z}] = \begin{bmatrix} -\phi' y \\ \phi' x - \kappa_x z \\ \kappa_x y \end{bmatrix} + \begin{bmatrix} 0 \\ 0 \\ 1 \end{bmatrix} + \begin{bmatrix} 0 \\ 0 \\ \epsilon_{3,3} \end{bmatrix}.$$

So the right side of (151) is

$$\mathbf{\Theta}[\mathbf{\Gamma}_z \mathbf{r} + \frac{\partial \overline{\mathbf{r}}}{\partial z} + \boldsymbol{\epsilon}_{,z}] = \begin{bmatrix} -\phi' y \cos\phi - \sin\phi\cos\beta(\phi' x - \kappa_x z) + \sin\phi\sin\beta(\kappa_x y + 1 + \epsilon_{33}) \\ -\phi' y \sin\phi + \cos\phi\cos\beta(\phi' x - \kappa_x z) - \cos\phi\sin\beta(\kappa_x y + 1 + \epsilon_{33}) \\ \sin\beta(\phi' x - \kappa_x z) + \cos\beta(\kappa_x y + 1 + \epsilon_{33}) - z \end{bmatrix}$$

Therefore, the displacement is

$$\Delta\boldsymbol{\zeta} = \begin{bmatrix} -y\phi'\int\cos(\phi' z)\mathrm{d}z - \cos\beta\int\sin(\phi' z)(\phi' x - \kappa_x z)\mathrm{d}z + \int\sin(\phi' z)\beta(\kappa_x y + 1 + \epsilon_{33})\,\mathrm{d}z \\ -y\phi'\int\sin(\phi' z)\mathrm{d}z + \cos\beta\int\cos(\phi' z)(\phi' x - \kappa_x z)\mathrm{d}z - \int\cos(\phi' z)\beta(\kappa_x y + 1 + \epsilon_{33})\,\mathrm{d}z \\ \int\beta(\phi' x - \kappa_x z)\mathrm{d}z + \cos\beta\int(\kappa_x y + 1 + \epsilon_{33})\,\mathrm{d}z - z \end{bmatrix} \quad (154)$$

The first term of the x-component is $-y\sin(\phi' z)$. The middle term of the x-component is found by substituting (145) and (147) into it:

$$\begin{aligned} &-\cos\beta\int\sin(\phi' z)(\phi' x - \kappa_x z)\mathrm{d}z \\ &\quad = -\cos\beta\left[\phi' x\int\sin(\phi' z)\mathrm{d}z - \int\sin(\phi' z)\kappa_x z\mathrm{d}z\right] \\ &\quad = -\cos\beta\left[\phi' x\int\sin(\phi' z)\mathrm{d}z - \frac{F_y}{EI_x}\int\sin(\phi' z)(Lz - z^2)\mathrm{d}z\right] \\ &\quad = -\cos\beta\left\{-x\cos(\phi' z) - \frac{F_y L}{EI_x}\left[-z\frac{\cos(\phi' z)}{\phi'} + \frac{\sin(\phi' z)}{\phi'^2}\right] + \frac{F_y}{EI_x}\left[-z^2\frac{\cos(\phi' z)}{\phi'} + 2z\frac{\sin(\phi' z)}{\phi'^2} + 2\frac{\cos(\phi' z)}{\phi'^3}\right]\right\}\Bigg|_0^z \end{aligned}$$

Therefore, the middle term of the x-component is

$$\begin{aligned} &-\cos\beta\int\sin(\phi' z)(\phi' x - \kappa_x z)\mathrm{d}z \\ &\quad = \cos\beta\left\{x[\cos(\phi' z) - 1] + \frac{F_y}{EI_x}\left[(z^2 - Lz)\frac{\cos(\phi' z)}{\phi'} + (L - 2z)\frac{\sin(\phi' z)}{\phi'^2} - 2\left(\frac{\cos(\phi' z)}{\phi'^3} - \frac{1}{\phi'^3}\right)\right]\right\} \end{aligned}$$

The last term of the x-component is found in like manner:

$$\begin{aligned} &\int\sin(\phi' z)\beta(\kappa_x y + 1 + \epsilon_{33})\mathrm{d}z \\ &\quad = \int\sin(\phi' z)\frac{F_y}{EI_x}\left(Lz - \frac{z^2}{2}\right)\left[\frac{F_y}{EI_x}(L - z)y + 1 + \epsilon_{33}\right]\mathrm{d}z \\ &\quad = \frac{F_y}{EI_x}\int\sin(\phi' z)\left(Lz - \frac{z^2}{2}\right)\left[\left(\frac{F_y L y}{EI_x} + 1 + \epsilon_{33}\right) - \frac{F_y y}{EI_x}z\right]\mathrm{d}z \end{aligned}$$

$$= \frac{F_y}{EI_x}\int \sin(\phi' z)\left[\left(\frac{F_y L y}{EI_x}+1+\epsilon_{33}\right)Lz-\left(\frac{3F_y L y}{EI_x}+1+\epsilon_{33}\right)\frac{z^2}{2}+\frac{F_y y}{2EI_x}z^3\right]\mathrm{d}z$$

Integrating, this x-component becomes

$$\begin{aligned}\int \sin(\phi' z)\beta(\kappa_x y+1+\epsilon_{33})\mathrm{d}z &= \frac{F_y}{EI_x}\left\{\left(\frac{F_y L y}{EI_x}+1+\epsilon_{33}\right)L\left[\frac{\sin(\phi' z)}{\phi'^2}-z\frac{\cos(\phi' z)}{\phi'}\right]_0^z\right.\\ &+\left(\frac{3F_y L y}{EI_x}+1+\epsilon_{33}\right)\left[\frac{z^2}{2}\frac{\cos(\phi' z)}{\phi'}-z\frac{\sin(\phi' z)}{\phi'^2}-\frac{\cos(\phi' z)}{\phi'^3}\right]_0^z\\ &+\left.\frac{F_y y}{2EI_x}\left[-z^3\frac{\cos(\phi' z)}{\phi'}+3z^2\frac{\sin(\phi' z)}{\phi'^2}+6z\frac{\cos(\phi' z)}{\phi'^3}-6\frac{\sin(\phi' z)}{\phi'^4}\right]_0^z\right\}\end{aligned}$$

The first term of the y-component is $y\cos(\phi' z)\big|_0^z$. The middle term of the y-component is

$$\begin{aligned}&\cos\beta\int \sin(\phi' z)(\phi' x-\kappa_x z)\mathrm{d}z\\ &= \cos\beta\left[\phi' x\int\cos(\phi' z)\mathrm{d}z-\int\cos(\phi' z)\kappa_x z\mathrm{d}z\right]\\ &= \cos\beta\left[\phi' x\int\cos(\phi' z)\mathrm{d}z-\frac{F_y}{EI_x}\int\cos(\phi' z)(Lz-z^2)\mathrm{d}z\right]\\ &= \cos\beta\left\{x\sin(\phi' z)-\frac{F_y L}{EI_x}\left[z\frac{\sin(\phi' z)}{\phi'}+\frac{\cos(\phi' z)}{\phi'^2}\right]_0^z+\frac{F_y}{EI_x}\left[z^2\frac{\sin(\phi' z)}{\phi'}+2z\frac{\cos(\phi' z)}{\phi'^2}-2\frac{\sin(\phi' z)}{\phi'^3}\right]_0^z\right\}\end{aligned}$$

Evaluating at the limits gives

$$\begin{aligned}&\cos\beta\int \sin(\phi' z)(\phi' x-\kappa_x z)\mathrm{d}z\\ &= \cos\beta\left\{x\sin(\phi' z)+\frac{F_y}{EI_x}\left[(z^2-Lz)\frac{\sin(\phi' z)}{\phi'}+\frac{L-(L-2z)\cos(\phi' z)}{\phi'^2}-2\frac{\sin(\phi' z)}{\phi'^3}\right]\right\}\end{aligned}$$

The last term of the y-component is found in like manner:

$$\begin{aligned}&-\int\cos(\phi' z)\beta(\kappa_x y+1+\epsilon_{33})\mathrm{d}z\\ &= -\int\cos(\phi' z)\frac{F_y}{EI_x}\left(Lz-\frac{z^2}{2}\right)\left[\frac{F_y}{EI_x}(L-z)y+1+\epsilon_{33}\right]\mathrm{d}z\\ &= -\frac{F_y}{EI_x}\int\cos(\phi' z)\left(Lz-\frac{z^2}{2}\right)\left[\left(\frac{F_y L y}{EI_x}+1+\epsilon_{33}\right)-\frac{F_y y}{EI_x}z\right]\mathrm{d}z\\ &= -\frac{F_y}{EI_x}\int\cos(\phi' z)\left[\left(\frac{F_y L y}{EI_x}+1+\epsilon_{33}\right)Lz-\left(\frac{3F_y L y}{EI_x}+1+\epsilon_{33}\right)\frac{z^2}{2}+\frac{F_y y}{2EI_x}z^3\right]\mathrm{d}z\end{aligned}$$

Integrating gives

$$
\begin{aligned}
-\int \cos(\phi' z)\beta(\kappa_x y + 1 + \epsilon_{33})\mathrm{d}z \;=\; & -\frac{F_y}{EI_x}\left\{\left(\frac{F_y L y}{EI_x} + 1 + \epsilon_{33}\right) L \left[z\frac{\sin(\phi' z)}{\phi'} + \frac{\cos(\phi' z)}{\phi'^2}\right]\Bigg|_0^z \right. \\
& - \left(\frac{3F_y L y}{EI_x} + 1 + \epsilon_{33}\right)\left[\frac{z^2}{2}\frac{\sin(\phi' z)}{\phi'} + z\frac{\cos(\phi' z)}{\phi'^2} - \frac{\sin(\phi' z)}{\phi'^3}\right]\Bigg|_0^z \\
& \left. + \frac{F_y y}{2EI_x}\left[z^3\frac{\sin(\phi' z)}{\phi'} + 3z^2\frac{\cos(\phi' z)}{\phi'^2} - 6z\frac{\sin(\phi' z)}{\phi'^3} - 6\frac{\cos(\phi' z)}{\phi'^4}\right]\Bigg|_0^z \right\}
\end{aligned}
$$

The z-component can be re-written using (147) and (145) as:

$$
\begin{aligned}
& \int \beta(\phi' x - \kappa_x z)\mathrm{d}z \;+\; \cos\beta \int (\kappa_x y + 1 + \epsilon_{33})\,\mathrm{d}z \\
& = \frac{F_y}{EI_x}\left[\phi' x L\frac{z^2}{2} - \left(\frac{\phi' x}{2} + \frac{F_y L^2}{EI_x}\right)\frac{z^3}{3} + \frac{3}{8}\frac{F_y}{EI_x}Lz^4 - \frac{F_y}{EI_x}\frac{z^5}{10}\right] + \cos\beta\left[\left(\frac{F_y L y}{EI_x} + 1 + \epsilon_{33}\right)z - \frac{F_y y}{EI_x}\frac{z^2}{2}\right]
\end{aligned}
$$

For evaluation purposes, a corner of the rubber block will be evaluated at the midspan, and a corner point and the centroid will be evaluated at the tip. The displacements in (154), evaluated at the points

$$
\mathbf{p} = (0.01, 0.025, 0.10)\,, \qquad \mathbf{p} = (0.01, 0.025, 0.20)\,, \quad \text{and} \quad \mathbf{p} = (0.0, 0.0, 0.2)
$$

are

$$
\Delta\boldsymbol{\zeta} = \begin{bmatrix} -8.41\,\mathrm{mm} \\ -14.54\,\mathrm{mm} \\ 1.13\,\mathrm{mm} \end{bmatrix}, \qquad \Delta\boldsymbol{\zeta} = \begin{bmatrix} 6.20\,\mathrm{mm} \\ -35.21\,\mathrm{mm} \\ 0.55\,\mathrm{mm} \end{bmatrix}, \qquad \Delta\boldsymbol{\zeta} = \begin{bmatrix} -10.13\,\mathrm{mm} \\ -15.61\,\mathrm{mm} \\ -1.52\,\mathrm{mm} \end{bmatrix}.
$$

These and other points are plotted in Figure 5 to depict the rubber block of Example 3 in its deformed condition.

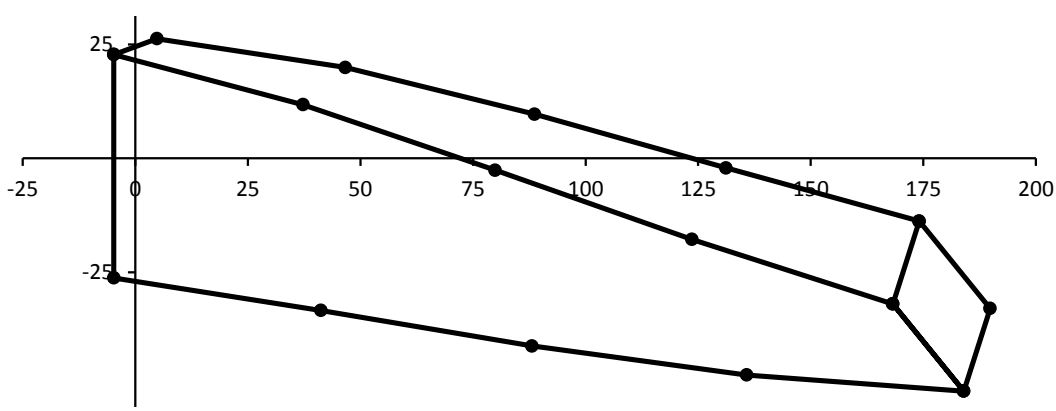

Figure 5. Reconstruction of rubber block of Example 3 (spatial units in mm).

The stress components derived above completely characterize the local state of stress; however, the von Mises stress, being proportional to the square root of the second invariant of the deviatoric stress tensor, represents the general multiaxial stress state by a single scalar invariant and so may be compared directly to the uniaxial yield strength obtained from standard tensile tests. Though not an appropriate yield criterion for rubber, it is useful here as a common scalar for comparing the stress solution with FEA studies. Figure 6 shows a plot of the von Mises stress, given by

$$\sigma_{\mathrm{VM}} = \sqrt{\frac{1}{2}\Big[(\sigma_{11}-\sigma_{22})^2+(\sigma_{22}-\sigma_{33})^2+(\sigma_{33}-\sigma_{11})^2\Big] + 3({\sigma_{12}}^2+{\sigma_{23}}^2+{\sigma_{31}}^2)}\,, \tag{155}$$

in the mid-section of the rubber block of Example 3. For this example, $\sigma_{11}=\sigma_{22}=\sigma_{12}=0$. The axial normal stress σ_{33}, which follows from (100), includes both the axial and bending contributions, with the bending curvature κ_x given by (145). The torsional shear stresses $\sigma_{13}^{(T)}$ and $\sigma_{23}^{(T)}$ are calculated from the Prandtl stress function in (125) and (126). The total shear stress σ_{23} also includes the bending contribution obtained from (104), which follows from integrating the closure condition (103) subject to zero shear traction at the boundaries of the rectangular cross-section. The factor κ_x' in (104) is computed from (145). The torsional and bending shear stresses are added algebraically as shown in (136), before evaluating the von Mises stress in (155). This gives:

$$\sigma_{33} = \frac{F_y\,(L-z)y}{I_x} + \frac{F_z}{W\,H}\,, \tag{156}$$

$$\sigma_{13} = \sigma_{13}^{(T)}\,, \qquad \sigma_{23} = \sigma_{23}^{(T)} + \frac{F_y}{2I_x}\left(\frac{H^2}{4}-y^2\right). \tag{157}$$

In this example, the torsional shear stresses generally dominate the bending and axial stress contributions.

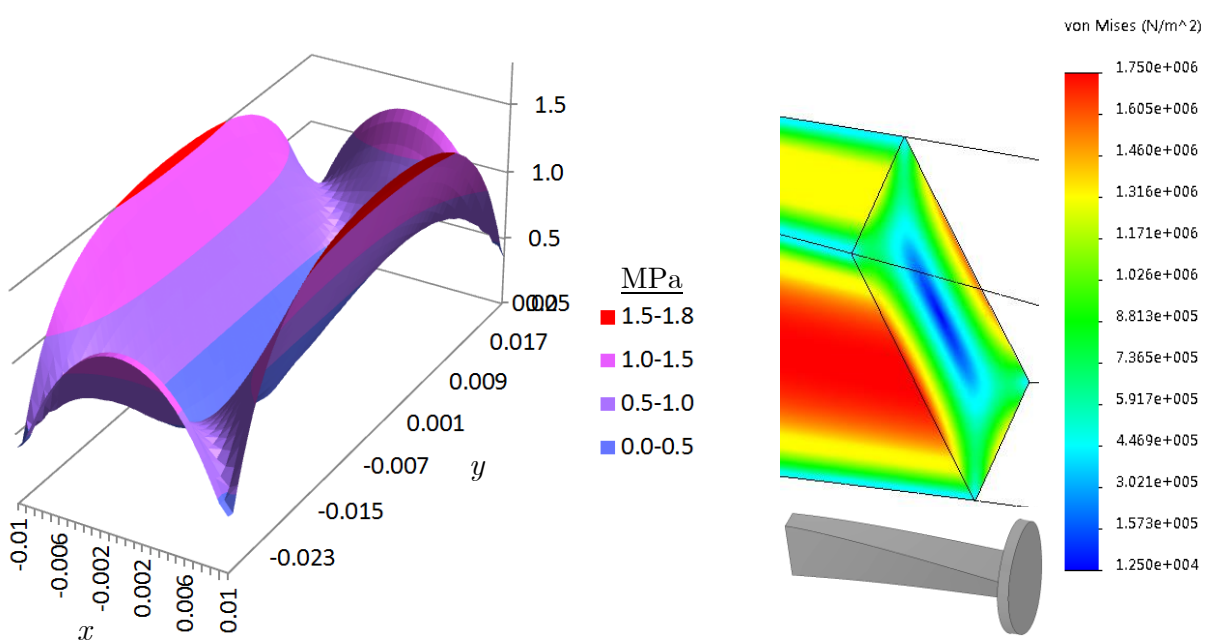

Figure 6. Surface plot of von Mises stress in the section at the mid-span ($z = 0.1\,\mathrm{m}$) of the rubber block of Example 3 under combined loading. (Right: SolidWorks FEA.)

Also shown in Figure 6 (right) are results of an FEA analysis of the same combined loads on the same rubber block (same G and E) using SolidWorks 2015. After the SolidWorks model began running, it prompted the user to use its Large Displacement option. But that option failed to converge during simulation, likely due to excessive displacements. Although subsequent versions of SolidWorks Simulation have introduced improvements in numerical solvers and nonlinear-analysis convergence, it is not known whether these improvements would resolve the convergence difficulty encountered here. The solution shown on the right in Figure 6 was obtained with its small displacement option (the default). As the figure legend shows, the max stress in that SolidWorks simulation is in good agreement with the analytical solution plotted with Excel (Figure 6, left). The max stress in the section is 1.74 MPa for SolidWorks and 1.71 MPa for the analytical solution. In order to apply an even torque distribution to the end face of the block, a rubber cylindrical hub was added to the model at the free end (shown in the lower right in Figure 6). The torque and axial compression boundary conditions were applied to this hub.

Although finite bending and torsional rotations do not commute, the difference between their two possible compositions is second order in the rotation angle. To leading order, the difference is

$$\mathbf{\Theta}_T \mathbf{\Theta}_B - \mathbf{\Theta}_B \mathbf{\Theta}_T \approx \begin{bmatrix} 0 & 0 & \phi\beta \\ 0 & 0 & 0 \\ \phi\beta & 0 & 0 \end{bmatrix}.$$

So the difference is proportional to the product of the bending and torsional angles. SolidWorks' linear static solution corresponds to neither finite rotation ordering in particular. It corresponds to the first-order approximation common to both.

3. Conclusion

The configuration of a body is represented in (3) as an SE(3)-valued field, with $\mathbf{\Theta} \in \mathrm{SE}(3)$, $\mathbf{a} \in \mathbb{R}^3$. The strain field $\boldsymbol{\xi}$ is an $\mathfrak{se}(3)$-valued Maurer–Cartan form:

$$\boldsymbol{\xi} = \begin{bmatrix} \mathbf{\Gamma} & \boldsymbol{\epsilon} \\ 0 & 0 \end{bmatrix},$$

that provides a geometrically exact representation of coupled rotational and translational deformation, consistent with established Cosserat and geometric rod theories. However, in classical SE(3)-based formulations, constitutive laws are typically defined directly on the Lie algebra-valued strain variables, without explicit incorporation of cross-sectional geometry at the constitutive level. In such approaches, sectional quantities such as bending and torsional stiffness arise only after separate spatial integration over the cross-section.

The present work introduced an additional affine coupling between this Lie-algebra strain and an intrinsic cross-sectional position field $\mathbf{R}$, leading to a strain measure of the form $\boldsymbol{\eta}_i = \mathbf{\Gamma}_{,i} \cdot \mathbf{R} + \boldsymbol{\epsilon}_{,i}$. The resulting strain measure embeds geometric structure directly into the constitutive level. This affine coupling led to classical sectional stiffness quantities, such as axial, bending, and torsional stiffness, emerging as geometric invariants of the affine strain field rather than as independently prescribed constitutive parameters. Warping and force–moment coupling arise naturally from this affine structure without introducing separate moment-arm constructions.

References

Antman, S. S., *Nonlinear Problems of Elasticity*, 2nd ed., Springer (2005).

Ball, R. S., *A Treatise on the Theory of Screws*, Cambridge University Press, Cambridge (1900).

Bloch, A. M., Nonholonomic Mechanics and Control, 2nd ed., Springer (2015).

Boresi, A. P. & Schmidt, R. J., *Advanced Mechanics of Materials*, 6th ed., Wiley, New Delhi (2003).

Bower, A. F., *Applied Mechanics of Solids*, CRC Press, Boca Raton (2010).

Brockett, R. W., "Some Mathematical Aspects of Robotics," in *Robotics, Proceedings of Symposia in Applied Mathematics* **41** (1990) pp. 1-19, American Mathematical Society, Providence, RI.

Cartan, E., "Sur la structure des groupes infinis de transformation," *Annales scientifiques de l'E.N.S.* **21** (1904) pp. 153-206.

Cartan, E., *Leçons sur la géométrie des espaces de Riemann*, Gauthier-Villars, Paris (1928).

Castigliano, A., *Theorie de I'equilibre des systemes elastiques et ses applications*, A. F. Negro, Turin, 480 pp. (1879); [translated into English as *Elastic Stresses in Structures*, by E. S. Andrews, Scott (1919); republished in 1966 as *The Theory of Equilibrium of Elastic Systems and Its Applications*, with a new introduction and biographical portrait by G. A. Oravas, Dover (1966)].

Cayley, A., "On the six coordinates of a line," *Transactions of the Cambridge Philosophical Society* **11** (1869) pp. 290–323.

Chevalley, C., *Theory of Lie Groups I*, Princeton University Press, Princeton, NJ (1946).

Chirikjian, G. S. & Kyatkin, A. B., *Engineering Applications of Noncommutative Harmonic Analysis: with Emphasis on Rotation and Motion Groups*, CRC Press, Boca Raton (2000).

Cosserat, E. & Cosserat, F., *Theorie des Corps Deformables*, Librairie Scientifique, Paris (1909); translated as *Theory of Deformable Bodies* by D. H. Delphenish.

Denavit, J. & Hartenberg, R. S., "A Kinematic Notation for Lower-Pair Mechanisms Based on Matrices," *Journal of Applied Mechanics* **22** (1955) pp. 215-221.

Eringen, A. C., *Microcontinuum Field Theories: I. Foundations and Solids*, Springer (1999).

Gere, J. M. & Timoshenko, S. P., *Mechanics of Materials*, PWS-Kent, Boston (1990).

Hante, S., Tumiotto, D., & Arnold, M., "A Lie group variational integration approach to the full discretization of a constrained geometrically exact Cosserat beam model," *Multibody System Dynamics* **54** (2021) pp. 97-123.

Harsch, J., Sailer, S., & Eugster, S. R., "A total Lagrangian, objective and intrinsically locking-free Petrov-Galerkin SE(3) Cosserat rod finite element formulation," *International Journal of Numerical Methods in Engineering* **124** (2023) pp. 2965-2994.

Helgason, S., *Differential Geometry, Lie Groups, and Symmetric Spaces*, Academic Press, New York (1978).

Helnwein, P., "Some remarks on the compressed matrix representation of symmetric second-order and fourth-order tensors," *Computer Methods in Applied Mechanics and Engineering* **190** (2001) pp. 2753-2770.

Ike, C. C., "Solving Saint Venant torsion problems for rectangular beams using single finite Fourier sine transform method," *Journal of Mechatronics and Artificial Intelligence in Engineering* **5** (2024) pp. 31-41.

Lynch, K. M. & Park, F. C., *Modern Robotics: Mechanics, Planning, and Control*, Cambridge University Press, Cambridge (2017).

Mandel, J., "Généralisation de la théorie de plasticité de WT Koiter," *International Journal of Solids and Structures* **1** (1965) pp. 273-295.

Mánik, T., "A natural vector/matrix notation applied in an efficient and robust return-mapping algorithm for advanced yield functions," *European Journal of Mechanics / A Solids* **90** (2021) pp. 104357-1-21.

Marsden, J. E. & Ratiu, T. S., *Introduction to Mechanics and Symmetry: A Basic Exposition of Classical Mechanical Systems*, 1st ed., Springer (1999); 2nd ed. (2010).

Murray, R. M. & Sastry, S. S., "Grasping and Manipulation using Multifingered Robot Hands," *Robotics, Proceedings of Symposia in Applied Mathematics* **41** (1990) pp. 91-127, American Mathematical Society, Providence, RI.

Murray, R. M., Li, Z., & Sastry, S. S., *A Mathematical Introduction to Robotic Manipulation*, CRC Press, Boca Raton (1994).

Park, F. C. & Brockett, R. W., "Kinematic Dexterity of Robotic Mechanisms," *The International Journal of Robotics Research* **13** (1994) pp. 1-15.

Paul, R. P., *Robot Manipulators: Mathematics, Programming, and Control*, MIT Press, Cambridge, MA (1981).

Reissner, E., "On One-Dimensional Large-Displacement Finite-Strain Beam Theory," *Studies in Applied Mathematics* **52** (1973) pp. 87-95.

Reissner, E., "On finite deformations of space-curved beams," *Journal of Applied Mathematics and Physics* (*ZAMP*) **32** (1981) pp. 734-744.

Saint-Venant, A. J. C. B. de, "Mémoire sur La Torsion des Prismes, Avec des Considérations sur leur flexion ainsi que sur L'équilibre intérieur des solides élastiques en général, et des formules pratiques pour le calcul de leur résistance à divers efforts s'exerçant simultanément," *Mémoires présentés par divers savants à l'Académie des Sciences de l'Institut de France* **14** (1856) pp. 234-560, 813-815.

Selig, J. M., *Geometric Fundamentals of Robotics*, 2nd ed., Springer (2005).

Simo, J. C., "A finite strain beam formulation. The three-dimensional dynamic problem. Part I," *Computer Methods in Applied Mechanics and Engineering* **49** (1985) pp. 55-70.

Simo, J. C. & Vu-Quoc, L, "A three-dimensional finite-strain rod model. Part II: Computational aspects," *Computer Methods in Applied Mechanics and Engineering* **58** (1986) pp. 79-116.

Simo, J. C. & Vu-Quoc, L., "A Geometrically-exact rod model incorporating shear and torsion-warping deformation," *International Journal of Solids and Structures* **27** (1991) pp. 371-393.

Sonneville, V., Cardona, A., & Brüls, O., "Geometrically exact beam finite element formulated on the special Euclidean group SE(3)," *Computer Methods in Applied Mechanics and Engineering* **268** (2014) pp. 451-474.

Surmont, F. & Coache, D., "Geometrically exact static 3D Cosserat rods problem solved using a shooting method," *International Journal of Non-Linear Mechanics* **119** (2020) 103330, 62 pp.

Till, J., Aloi, V., & Rucker, C., "Real-time dynamics of soft and continuum robots based on Cosserat rod models," *The International Journal of Robotics Research* **38** (2019) pp. 1-24.

Vardoulakis, I., *Cosserat Continuum Mechanics With Applications to Granular Media*, Springer (2019).

Voigt, W., *Lehrbuch der Kristallphysik*, Teubner, Leipzig (1910).

Weeger, O., Yeung, S.-K., & Dunn, M. L., "Isogeometric collocation methods for Cosserat rods and rod structures," *Computer Methods in Applied Mechanics and Engineering* **316** (2017) pp. 100-122.

Xun, L. & Tamadazte, B., "Geometrically Explicit Cosserat-Rod Modeling with Piecewise Linear Strain for Complex Rod Systems," *Computers & Structures* **325** (2026) 108181.

Young, W. C., & Budynas, R. G., *Roark's Formulas for Stress and Strain*, 7th ed., McGraw-Hill, New York (2002).